

## Holocene and Anthropocene Landscape Change: Arroyo Formation on Santa Cruz Island, California

Ryan L. Perroy , Bodo Bookhagen , Oliver A. Chadwick & Jeffrey T. Howarth

To cite this article: Ryan L. Perroy , Bodo Bookhagen , Oliver A. Chadwick & Jeffrey T. Howarth (2012) Holocene and Anthropocene Landscape Change: Arroyo Formation on Santa Cruz Island, California, *Annals of the Association of American Geographers*, 102:6, 1229-1250, DOI: [10.1080/00045608.2012.715054](https://doi.org/10.1080/00045608.2012.715054)

To link to this article: <https://doi.org/10.1080/00045608.2012.715054>



Published online: 17 Sep 2012.



Submit your article to this journal [↗](#)



Article views: 579



View related articles [↗](#)



Citing articles: 13 View citing articles [↗](#)

# Holocene and Anthropocene Landscape Change: Arroyo Formation on Santa Cruz Island, California

Ryan L. Perroy,\* Bodo Bookhagen,<sup>†</sup> Oliver A. Chadwick,<sup>†</sup> and Jeffrey T. Howarth<sup>‡</sup>

\*Department of Geography and Earth Science, University of Wisconsin–La Crosse

<sup>†</sup>Department of Geography, University of California at Santa Barbara

<sup>‡</sup>Department of Geography, Middlebury College

In this study, we untangle the relative importance of climatic, tectonic, and anthropogenic drivers as triggers of arroyo formation and geomorphic change for a small watershed on Santa Cruz Island, California. Within the Pozo watershed (6.47 km<sup>2</sup>), historic arroyo incision occurred contemporaneously with arroyo incision across many of the world's dryland regions. Unlike many of these other sites, Pozo contains a datable record that allows quantification of sedimentation rates from the mid-to-late Holocene to the twentieth century. Basin-wide environmental changes were assessed using a combination of cosmogenic radionuclide inventories, midden and marine-shell deposits, relict soil properties, airborne and ground-based light detection and ranging (lidar) data, ranching artifacts, and historic records. Shortly after the introduction of sheep in 1853, localized sedimentation rates on the Pozo floodplain increased by two orders of magnitude from 0.4 mm/year to ~25 mm/year. Accelerated sedimentation was followed by arroyo formation ca. 1878 and rapid expansion of the incipient gully network, the lateral extent of which has been largely maintained since 1929. Catchment-mean erosion rates from cosmogenic radionuclide measurements indicate that presettlement rates were less than 0.08 mm/year, whereas lidar-derived measurements of historic gully erosion produce estimates almost thirty times higher (~2.2 mm/year). Topographic measurements since 2005 indicate that the active channel of the Pozo watershed is aggrading. We argue that accelerated sedimentation due to overgrazing, and an unusually large 1878 rainstorm event, set the stage for arroyo formation in the Pozo watershed between 1875 and 1886. We hypothesize that even in the absence of modern human disturbance, downcutting would have occurred due to intrinsic hillslope stability thresholds. *Key Words:* cosmogenic radionuclides, gully incision, lidar, overgrazing.

我们将在本研究中解开气候、地壳构造与人类驱动力在触发加州斯塔克鲁兹岛上小型流域旱谷生成与地形变迁的相对重要性。在波索流域 (6.47平方公里) 中, 历史性的旱谷切蚀与世界上许多旱地区的旱谷切蚀同时发生。但有别于其他地方, 波索流域保有着可追溯年代的纪录, 因此可对自全新纪中、晚期至二十世纪以来的沉降率进行量化工作。本研究结合了宇宙放射性核素值、贝丘与海洋贝壳沉积、残余土壤组成、空中与地面激光探测、一系列的激光 (雷达) 数据, 以及牧场人造物与历史纪录, 对全流域的环境变迁进行评估。1853年引进羊群不久之后, 波索冲积平原的地方沉降率增加了两个数量级—自每年0.4公厘增加至每年约25公厘。尾随加速沉积而至的, 便是约在1878年间旱谷的形成, 以及原本沟蚀网络的快速扩张, 其中的横向范围自1929年来便大幅保存下来。宇宙放射性核素方法所测得的流域平均侵蚀率显示, 在屯垦之前每年仅有少于0.08公厘的侵蚀率, 而透过激光 (光学) 雷达方法所估计的历史性沟蚀则几乎高出三十倍 (约每年2.2公厘)。自2005年以来的地形测量方法指出, 波索流域的流水河槽正在升高。我们认为, 加速的沉积是由过度放牧和1878年一起不寻常的暴雨事件所造成, 导致波索流域1875年至1886年间的旱谷形成。我们提出以下假设: 即使没有现代人类的干扰, 仍会因为山坡稳定性的固有门坎而发生下蚀作用。关键词: 宇宙放射性核素, 沟蚀, 激光 (光学) 雷达, 过度放牧。

En este estudio rescatamos la importancia relativa que tienen los factores climáticos, tectónicos y antropogénicos como fuerzas que inician la formación de arroyos y el cambio geomórfico en una pequeña cuenca hidrográfica de la Isla de Santa Cruz, en California. En la cuenca del Pozo (6.47 km<sup>2</sup>), el excavado histórico de arroyos ocurrió contemporáneamente con procesos similares que afectaron a muchas de las regiones áridas del mundo. A diferencia de lo que ocurre en muchos de estos otros lugares, el Pozo contiene un registro susceptible de datación que permite la cuantificación de tasas de sedimentación desde el Holoceno medio y tardío hasta el siglo XX. Los cambios ambientales ocurridos en toda la cuenca se calcularon utilizando una combinación de inventarios radionúclidos cosmogénicos, basureros y concherías marinas, propiedades de relictos pedológicos, datos sobre detección y ámbito de luminosidad (LIDAR) desde el aire y a nivel del suelo, artefactos usados en los ranchos

ganaderos y registros históricos. Poco después de la introducción de las ovejas en 1853, las tasas de sedimentación de la llanura inundable del Pozo se incrementaron en dos órdenes de magnitud, desde 0.4 mm/año a ~25 mm/año. A la sedimentación acelerada siguió hacia 1878 la formación de arroyos, lo mismo que una rápida expansión de la incipiente red de cárcavas, cuya extensión lateral se ha mantenido en gran medida desde 1929. Las tasas de erosión media por unidad de demarcación tomadas de las mediciones de radionúclidos cosmogénicos indican que las tasas anteriores al poblamiento fueron de menos de 0.08 mm/año, en tanto que las medidas de la erosión histórica en cárcavas derivadas del LIDAR producen estimativos casi treinta veces más altos (~2.2 mm/año). Las mediciones topográficas a partir del 2005 indican que el canal activo de la cuenca del Pozo se halla en proceso de agradación. Creemos que la sedimentación acelerada debida al sobrepastoreo, más una inesperada gran tormenta de 1878 pusieron en marcha el proceso de formación de arroyos en la cuenca del Pozo entre 1875 y 1886. Nuestra hipótesis es que aun si se prescindiera de las perturbaciones modernas de origen antrópico, la erosión en cárcavas habría ocurrido debido a los intrínsecos umbrales de estabilidad de las laderas. *Palabras clave:* radionúclidos cosmogénicos, incisión de cárcavas, LIDAR, sobrepastoreo.

**M**ajor global increases in erosion and sedimentation rates over the past few centuries to millennia, often attributed to human activity, variations in climate, or tectonic events, have altered previously stable landscapes around the world (Allen and Breshears 1998; Zhang, Molnar, and Downs 2001; Dadson et al. 2003; Lal 2003; Bayon et al. 2012) and caused extensive environmental disruption and degradation worldwide (Montgomery 2007; Bai et al. 2008). Depending on their levels of sensitivity and the time periods involved, disrupted landscapes can form new equilibrium states or maintain unstable transient forms. A more thorough understanding of landscape stability thresholds is needed to predict the magnitude and direction of current and future changes associated with both land management and climate change (Goudie 2006).

A key example of landscape instability is the nineteenth-century wave of arroyo incision that rolled across the world's semiarid rangelands (Cooke and Reeves 1976). An *arroyo* is an entrenched stream channel in cohesive valley-floor alluvium characterized by steep vertical walls (Bull 1997). Throughout the century, the sequence of land-cover change, accelerated floodplain sedimentation, and arroyo/gully incision repeatedly dropped water tables, damaged infrastructure, and desertified millions of acres of rangeland globally throughout semiarid regions in the American Southwest (Cooke and Reeves 1976; Waters and Haynes 2001), Australia (Fanning 1999; Prosser et al. 2001), and southern Africa (Fox 2000) but also in the more humid American upper Midwest (Knox 1977, 1987, 2006).

The process of arroyo formation, from initial incision to channel widening and possible reaggradation, is fairly well understood (Leopold and Miller 1956; Schumm and Hadley 1957; Elliott 1979; Schumm, Harvey, and

Watson 1984). Previous studies examining the causes of arroyo formation have focused on factors such as climate (Antevs 1952; Waters and Haynes 2001; Hereford 2002; McAuliffe, Scuderi, and McFadden 2006), land use (Dodge 1902; Bryan 1925; Meyer 1986; Patton and Boison 1986; Fanning 1999), and intrinsic geomorphic thresholds (Schumm and Parker 1973; Patton and Schumm 1981; Elliott, Gellis, and Aby 1999). Soils and vegetation, which bridge the different factors at various scales (Bull 1997; Marston 2010), also play a critical role in conditioning geomorphic change and arroyo formation.

Although evidence for these factors is compelling, few studies have been able to reconstruct or measure the interaction of these factors for a particular landscape at the moment it reaches its stability threshold. For most of these studies, unrecorded or unavailable data create uncertainty about causality. For example, Fanning (1999) argued persuasively that introduced domestic and feral herbivores were responsible for arroyo cutting in western New South Wales, Australia, but the study could not rule out the influence of climate due to a lack of local precipitation data. In other cases, missing important details included long-term geologic and baseline erosion rates, exact timing of arroyo incision, detailed precipitation data, and precise records of grazing pressures and other human land-use decisions. Arroyo formation represents a complex response often initiated by the collision of human land use and climate variability; sites with a preserved record of these variables over relevant timescales are rare.

Here we present data from the Pozo watershed on southwestern Santa Cruz Island (SCI), California. This particular watershed, along with the entire island, has undergone a series of well-documented and intensive changes in land-use history since the mid-nineteenth century, culminating in its present incarnation as a

nongrazed natural preserve. We have taken advantage of this history, and the island's relative isolation and wealth of exposed datable stratigraphic markers dating back to the mid-Holocene, to quantify the processes of arroyo formation in a previously stable landscape.

Our approach is threefold and combines records encompassing different spatial and temporal scales. First, we establish rates of baseline environmental processes over long (>5 ky [thousand years]) timescales and large spatial scales (>10 km<sup>2</sup>). These records include published tectonic uplift rates and eustatic sea-level change data, sedimentary and archaeological data from SCI and neighboring Santa Rosa Island (SRI), and cosmogenic nuclide catchment-mean erosion rates for the Pozo watershed. Over long timescales and at large spatial scales, geologic uplift rates and sea-level changes are the main driving forces for this landscape, although paleoclimatic changes also play a role. Second, we examine historical archives and artifacts to determine the timing and magnitude of recent geomorphic events and drivers during the past two centuries. These records, including sheep stocking rates, repeated topographic surveys, and precipitation data, provide insight into the rapid geomorphic changes that occurred in the mid-to late-nineteenth century. Third, we use high-spatial-resolution light detection and ranging (lidar) data to estimate erosion rates in the postgrazing landscape via volumetric loss estimates of historic gullying. We then compare these historic erosion estimates to long-term pregrazing rates derived from cosmogenic nuclide and other measurements. Taken together, these data sets provide one of the most complete and detailed studies of arroyo formation currently available (Figure 1).

## Geographic, Climatic, and Geologic Setting of Santa Cruz Island

The largest of the California Channel Islands, SCI is located 38 km off the California central coast at 34° N, 119°45' W (Figure 2). It is roughly 37 km long east to west and ranges from 3 km to 11 km wide north to south. Topographic relief on the island is high (>0.75 km in a 5-km radius) and the geologic evolution complex, featuring a mixture of terrestrial and marine sediments and magmatic deposits, bounded by several tectonically active faults (Weaver and Nolf 1969; Dibblee 2001). SCI is part of the tectonically active Transverse Ranges; the island has experienced long-term uplift rates estimated at 0.7 to 1.5 mm/year (Pinter, Sorlien, and Scott

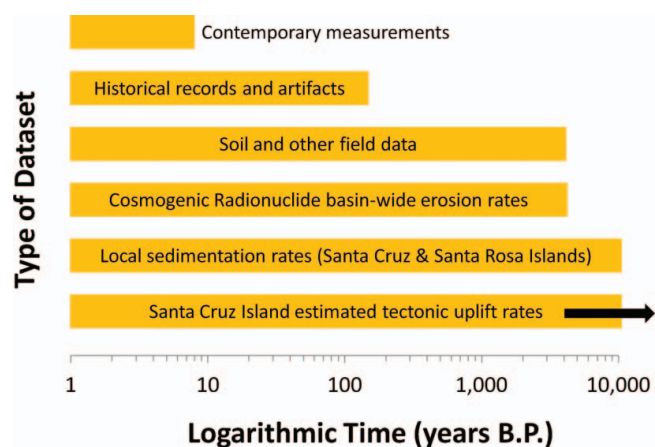


**Figure 1.** Synthesis of data sets and their corresponding temporal resolution used in this study. Length of bars indicates relevant time span each data set covers. Santa Cruz Island tectonic uplift rates are taken from uplifted marine terraces and submerged paleoshorelines (Pinter, Sorlien, and Scott 2003; Chaytor et al. 2008); local sedimentation rates are compiled from Cole and Liu (1994), Ballantyne (2006), Glassow et al. (2009), and this study. (Color figure available online.)

2003; Chaytor et al. 2008). On millennial and longer timescales, the long-term tectonic uplift rate results in the formation of marine wave-cut platforms that characterize some coastal areas of SCI and elsewhere along California's coast.

Since the last glacial maximum at ~21 ka (Fairbanks 1989; Bard et al. 1990), sea-level rise drastically changed California's coastline, inundating vast areas and reducing the former super-island of Santarosae to its present four constituent islands: San Miguel, Santa Rosa, Santa Cruz, and Anacapa (Nardin et al. 1981; D. L. Johnson 1983; Porcasi, Porcasi, and O'Neill 1999). Inundation increased the effective base level of many streams and temporarily created estuaries in coastal valleys that subsequently backfilled with sediment as the rate of sea-level rise slowed (Bickel 1978; Inman 1983; Graham, Dayton, and Erlandson 2003). Similar observations on analogous islands in south-central Chile suggest that stable sea levels since ~6 ka created an aggrading environment that allowed sediments to record ongoing tectonic events (Bookhagen et al. 2006).

This study was conducted within the 6.47 km<sup>2</sup> Pozo watershed on the southwestern corner of SCI (Figure 2). Geologically, the basin can be divided into three broad zones: The western section is made up of a series of exposed and weakly lithified upper Miocene sedimentary formations; the middle part is composed of the moderately resistant San Onofre breccias; and the eastern

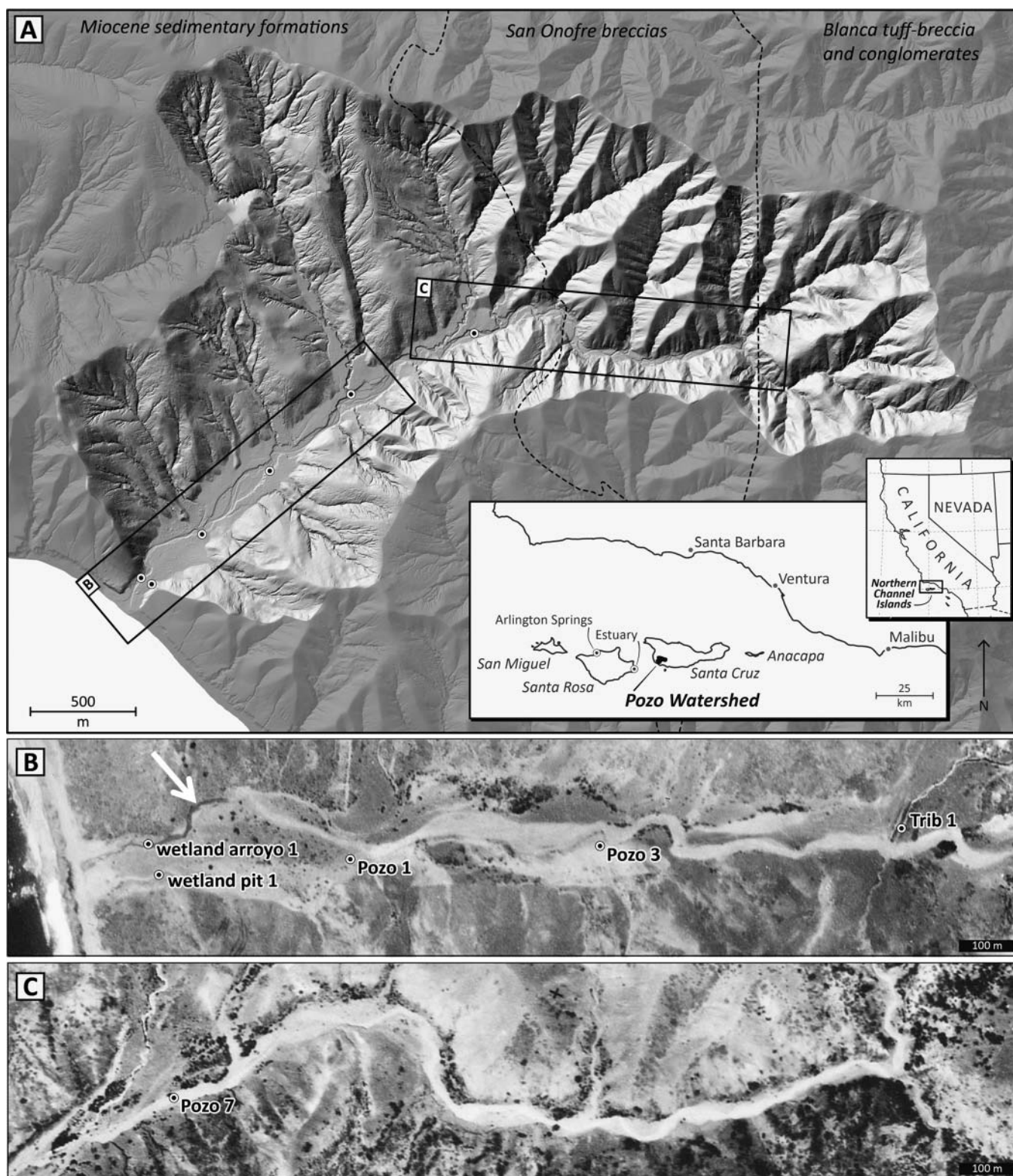


**Figure 2.** Study site. (A) Hillshade relief image of Pozo watershed showing sedimentation sampling sites (round markers), generalized geology (modified from Weaver and Nolf 1969), and inset locator map for Pozo watershed and the Northern Channel Islands (Santa Rosa Island sedimentation sampling sites also shown). (B) 1929 aerial image of lower Pozo channel and sedimentation sampling sites. Perennially wet channel indicated by white arrow. (C) 1929 aerial image of upper Pozo channel and Pozo 7 sedimentation sampling site. 1929 orthomosaic provided by Molander and Pinter, Southern Illinois University.

section is composed of the Blanca formation, a series of more resistant tuff-breccia and conglomerate units. Soils in the canyon are primarily Entisols, Mollisols, and Vertisols, with Argixerolls, Chromoxererts, and Haploxerolls on the soil-mantled hillslopes (U.S. Department of Agriculture 2007). Floodplain soils are thick, dark, and fine-grained (Cumulic Haploxerolls), buried in many places by a historically deposited buff-colored layer of sediment (Brumbaugh 1980, 1983; Glassow et al. 2009). Landscape morphology and land cover in the basin varies from rolling grass-covered hills of the western section to scattered stands of Bishop pine (*Pinus muricata*) and ironwood (*Lyonothamnus floribundus*) and rugged exposed bedrock in the eastern section. Gully and erosion scars are prevalent throughout the basin but are most common in the western section. The soil within the active channel of Pozo watershed is perennially wet from the mouth to a distance upstream of 300 to 500 m, a condition visible in every aerial photograph taken of southwestern SCI dating back to 1929 (Figure 2B).

The island has a Mediterranean climate characterized by warm, dry summers and cool, moist winters. Average annual temperature is 16°C to 23°C, varying primarily by elevation. Average annual precipitation is 511 mm with a recorded maximum of 1,426 mm, based on a 106-year record from the island main ranch. The rainy season falls between October and April and it is strongly affected by the El Niño Southern Oscillation (Pinter and Vestal 2005).

## Historic Context and Anthropogenic Setting

The earliest evidence for human occupation of SCI comes from Chumash Indian cultural artifacts, dating as early as 8,700 cal yr BP (Glassow 2002). Chumash influence on the terrestrial ecology and geomorphology of SCI is not clear, aside from limited evidence of prescribed burning (Timbrook, Johnson, and Earle 1982; Timbrook 1993). Disturbance under the Chumash was likely minimal compared to the events following the introduction of grazing livestock (Erlandson, Rick, and Vellanoweth 2004; Kennett 2005; Glassow et al. 2009). The first report of livestock on SCI dates from April 1830, when thirty-one Mexican prisoners were left briefly on the island, “the mission furnishing some tools, cattle, hooks, and a little grain” (Bancroft 1886, 48). In 1851, U.S. Coast Survey Lieutenant Commander James Alden noted, “There are a few cattle here [on SCI], but,

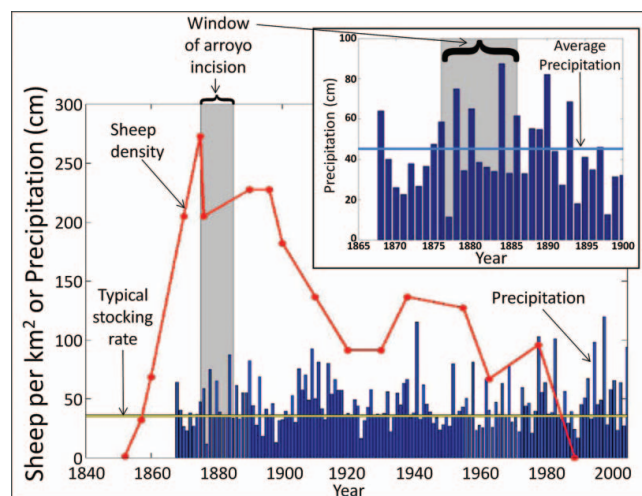


**Figure 3.** Comparison of Santa Cruz Island sheep-density estimates and precipitation data from the city of Santa Barbara (~50 km away). Sheep-density estimates gathered from a variety of sources, with round-ups being the most problematic ones as they might only capture about 50 percent of the actual population (Symmes and Associates 1922). Typical mainland sheep stocking rate is shown for comparison. Historic maps of Pozo watershed used to bound arroyo incision window. Upper right inset image of arroyo incision window shows dramatic 1877 drought, followed by heavy 1878 rains (likely date for arroyo incision). (Color figure available online.)

like the other islands, there are no inhabitants” (Alden 1853, 105–06). In 1852, a squatter raised pigs on SCI and left the following year, when ranching activities began in earnest (U.S. District Court 1857). By 1853, the list of introduced livestock included sheep (*Ovis aries*), cattle (*Bos taurus*), pigs (*Sus scrofa*), and horses (*Equus ferus caballus*), with sheep probably responsible for most of the soil degradation and erosion that followed (Brumbaugh 1983; Van Vuren and Coblentz 1987; Schuyler 1993; Howarth and Laughrin 2009). Wood cutting for timber or firewood (Spaulding 1964; Hochberg, Junak, and Philbrick 1980) and rooting feral pigs (Roemer, Donlan, and Courchamp 2002; Ramsey, Parkes, and Morrison 2009) also likely played a role. Estimates of SCI’s sheep population in the latter half of the 1800s reveal unsustainable growth (Figure 3), with the population rising from a small number of introduced sheep in 1853 to 45,000 sheep in 1870 (U.S. Bureau of the Census 1870). Fencing was not extensively used in this early period and livestock were generally allowed free range over the entire island (Howarth and Laughrin 2009).

Problems associated with sheep overpopulation, including erosion due to overgrazing (Figure 4), eventually became so severe that sheep removal efforts began as early as 1939 (Junak et al. 1995). Tens of

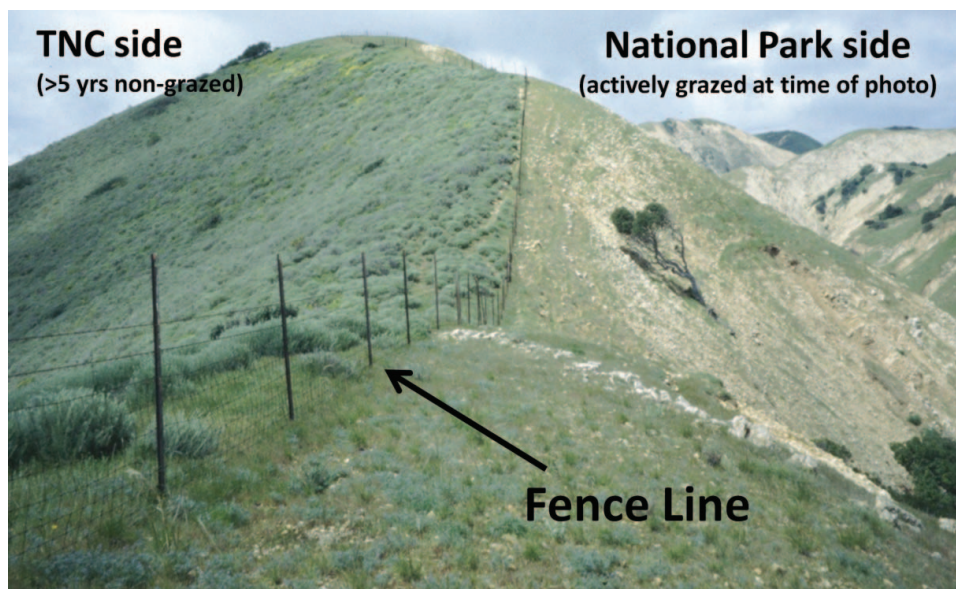


**Figure 4.** Overgrazing-induced erosion and the vegetation boundary effect of fence lines. This photograph was taken in the mid-1990s near The Nature Conservancy (TNC; left)–National Park (right) border on Santa Cruz Island. At the time of the photo, TNC land had already experienced several years of recovery in the absence of grazing. Photograph by J. Howarth. (Color figure available online.)

thousands of sheep were rounded up or shot in the following decades as part of removal efforts (Van Vuren 1981). Between the years 1956 and 1962 alone, 24,000 sheep were removed from SCI (Howarth and Laughrin 2009). The Nature Conservancy and National Park Service eventually acquired ownership of SCI and began a livestock removal program. Cattle were removed from SCI in 1988, sheep by 2001 (Faulkner and Kessler 2011), and island-wide pig removal efforts were completed in 2007 and 2008, completing the eradication of introduced livestock.

These land-use changes (the introduction of grazing animals, establishment of a large feral sheep population, and subsequent eradication) dramatically affected the island's vegetation. Although little quantitative vegetation information exists for the pregrazing period, written accounts, mid-nineteenth-century photos of densely wooded ridgelines, and the remains of dead root burls and downed trunks attest to an earlier period of markedly denser vegetative cover (Greenwell 1857; W. M. Johnson 1860; Brumbaugh 1983; Junak et al. 1995). Introduced livestock severely suppressed and modified coastal sage scrub (*Artemisia californica*, *Eriogonum* spp., *Salvia mellifera*, *Encelia californica*), island chaparral (*Quercus dumosa*, *Cercocarpus betuloides*, *Prunus lyonii*, *Rhus integrifolia*, *Adenostoma fasciculatu*, and others), valley and foothill grassland (*Avena* spp., *Bromus* spp., and *Hordeum* spp.), and oak woodland (*Quercus agrifolia*/*Quercus pacifica*) communities across

the island (Brumbaugh 1980). With the removal of livestock, vegetation recovery has proceeded to the point of lessening slope failures (Gabet and Dunne 2002; Pinter and Vestal 2005), and aggressive nonnative species, including fennel (*Foeniculum vulgare*) and yellow star thistle (*Centaurea solstitialis*) have now colonized much of the island (Hochberg, Junak, and Philbrick 1980; Junak et al. 1995; Colvin and Gliessman 2000).

## Materials and Methods

To understand and quantify the causes, magnitude, and timing of arroyo formation and associated watershed changes in Pozo canyon, we collected four types of data: (1) field data, (2) historic documents and maps, (3) cosmogenic radionuclide (CRN)  $^{10}\text{Be}$  measurements, and (4) topographic data. Our strategy in combining these disparate data sets was to produce as complete a record of geomorphic change as possible from the mid-Holocene to the present.

### Field Data: Local Sedimentation Rate Calculations from Datable Sedimentary Markers

To calculate changes in local sedimentation rates, we included only sites containing multiple datable sedimentary markers. We visually identified and surveyed sites in the field in addition to gathering data from previous studies (Cole and Liu 1994; Ballantyne 2006;

Glassow et al. 2009; J. Johnson, personal communication, 29 May 2009). More than forty datable markers were collected and dated across seven different sites on SCI and SRI (Figure 2, Table 1). To our knowledge, the sites described in this study are the only locations on southwestern SCI that contain multiple datable markers and include all published and unpublished accounts of multiple datable markers on SRI, although additional sites might exist on that island. Markers included land surfaces, soil horizon contacts, and fluvial deposits containing mussel and abalone shells (presumably from Chumash Indian shell middens), charcoal fragments, soil organic matter, and ranching artifacts. Markers containing carbon were dated via conventional or accelerator mass spectrometry (AMS) radiocarbon techniques (Beta Analytic). Radiocarbon dates from the SRI Arlington Springs archeological site (Orr 1962) were derived from humic acids and shell fragments within a soil core prepared and analyzed by Tom Stafford following the conventions of Stuiver and Polach (1977). If no shell was large enough by itself for a radiometric date, several fragments from the same stratum made up the sample. For some of the more recent markers, we used historic artifacts, documents, or both, including maps and ranching records to provide age control. Local sedimentation rates were calculated from marker ages (calibrated radiocarbon intercept or other ages) and hand-measured depths between strata at the same site (Figure 5). Minimum and maximum possible sedimentation rates were also calculated using the  $1\sigma$  dating errors (Figure 6).

We documented soil properties for each of the four Pozo midden sites, twelve additional sampling locations along the length of the Pozo arroyo, five soil pits across the lower Pozo floodplain, and more than 100 hand-augur sampling sites across the entire valley. Soil data from Pozo midden Site 1, wetland arroyo wall Site 1, and wetland soil pit 1 are shown in Table 2. We also recorded hydric and relict hydric soil properties where present, including the presence of redoximorphic features and gleyed soil matrix colors. Full profile descriptions of the other Pozo midden sites can be found in Glassow et al. (2009).

### Historic Documents and Maps

Historic documents and maps provide additional evidence for understanding landscape and land-use change on southwestern SCI following European contact and

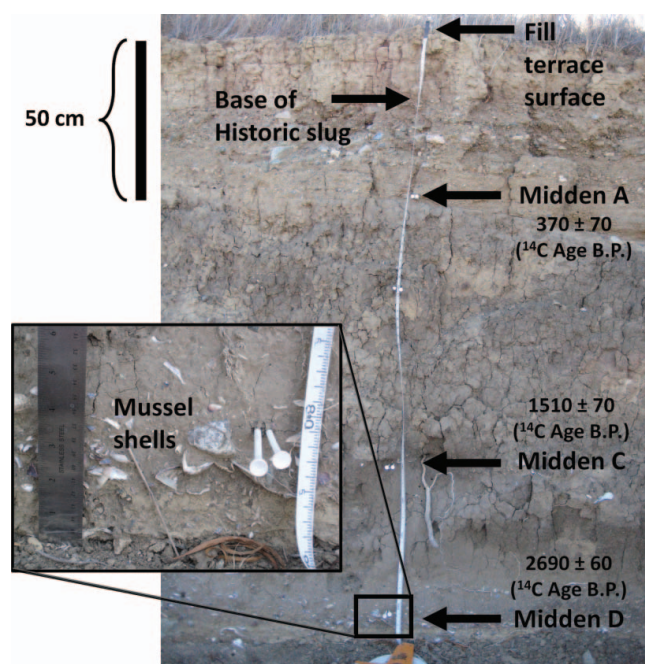


**Figure 5.** Pozo 1 site arroyo wall profile with datable markers including both sedimentary contacts (ages derived from historic materials) and midden shells (ages derived from radiocarbon intercepts). Trench containing additional dated *Mytilus ca.* shell below this profile not shown. (Color figure available online.)

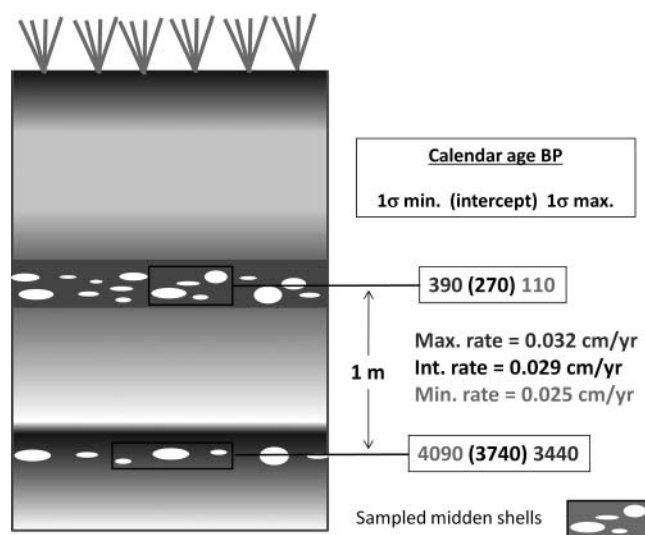


**Figure 6.** Conceptual arroyo wall exposure of midden strata for sedimentation rate calculation. The measured distances between midden strata are assumed to account for all of the sedimentation that has taken place in between times of midden deposition. The possibility of intervening scour events suggests that calculated sedimentation rates should be interpreted as minimum rates, but we have not found evidence for intermittent scouring events.

Table 1. Datable markers used to calculate local sedimentation rates

Site	Lab no.	Study	Stratigraphic marker <sup>a</sup>	Material	Depth (m)	C-14 age BP	Conv. age BP	Cal. age BP intercept & 1 sigma interval	Sedimentation rate <sup>b</sup> (mm/year)
Pozo 1	—	1	Fill terrace surface	Fill terrace surface	0	—	—	69 (64) 59	—
	—	1	Base of historic sediment	Historic sediment lower contact	0.28	—	—	120 (100) 80	7.8
Beta-185929		2	Pozo 1, Midden A	Several <i>Mytilus ca.</i> shells	0.56	370 ± 70	790 ± 70	390 (250) 40	1.9
Beta-185931		2	Pozo 1, Midden C	Several <i>Mytilus ca.</i> shells	1.4	1,510 ± 70	1,950 ± 70	1,420 (1,280) 1,130	0.8
Beta-185932		2	Pozo 1, Midden D	Several <i>Mytilus ca.</i> shells	1.9	2,690 ± 60	3,130 ± 70	2,830 (2,710) 2,450	0.3
Beta-246922		1	Trench at profile base	1 <i>Mytilus ca.</i> shell	2.45	3,380 ± 40	3,790 ± 40	3,520 (3,450) 3,400	0.7
Pozo 3	—	1	Fill terrace surface	Fill terrace surface	0	—	—	69 (64) 59	—
	—	1	Buried water pipe	Metal pipe	0.72	—	—	96 (92) 88	25.7
Beta-194823		2	Pozo 3, Midden A	1 <i>Haliotis cracherodii</i> shell	1	400 ± 50	830 ± 50	390 (270) 110	1.6
Beta-194824		2	Pozo 3, Midden B	1 <i>Mytilus ca.</i> shell	2.4	3,620 ± 120	4,030 ± 120	4,090 (3,740) 3,440	0.4
Pozo 7	—	1	Fill terrace surface	Fill terrace surface	0	—	—	69 (64) 59	—
	—	1	Base of historic sediment	Historic sediment lower contact	0.5	—	—	120 (100) 80	13.9
Beta-194826		2	Pozo 7, Midden B	5 <i>Mytilus ca.</i> shells	1.5	540 ± 70	950 ± 70	500 (390) 250	3.4
Beta-194827		2	Pozo 7, Midden C	5 <i>Mytilus ca.</i> shells	2.9	1,750 ± 40	2,160 ± 40	1,600 (1,500) 1,370	1.3
Beta-194828		2	Pozo 7, baking pit	Approx. 20 pieces of charcoal	4.75	2,460 ± 50	2,870 ± 50	2,470 (2,330) 2,180	2.2
Trib 1	—	1	Fill terrace surface	Fill terrace surface	0	—	—	69 (64) 59	—
Beta-185933		2	Trib 1, Strat B	Several <i>Mytilus ca.</i> and <i>Septifer bifurcatus</i> shells	4.1	2,680 ± 70	3,110 ± 70	2,790 (2,700) 2,400	1.6
Beta-185934		2	Trib 1, Strat C	Several <i>Mytilus ca.</i> and <i>Septifer bifurcatus</i> shells	5	3,440 ± 100	3,860 ± 100	3,820 (3,540) 3,310	1.1

Christi 1	—	3	Fill terrace surface	0	—	—	105 (90) 75
Beta-187392	3	Midden Stratum 2	Surface	0.3	—	1,740 ± 40	1,180 (1,060) 950
Beta-187393	3	Midden Stratum 6	Shell	1.2	—	2,460 ± 40	1,950 (1,840) 1,710
Beta-187394	3	Midden Stratum 8	Shell	1.7	—	2,940 ± 40	2,600 (2,360) 2,310
Beta-187395	3	Midden Stratum 16	Shell	4.9	—	4,110 ± 40	3,980 (3,850) 3,710
Beta-187396	3	Midden Stratum 18	Shell	5.5	—	4,370 ± 40	4,370 (4,220) 4,080
Beta-187924	3	Midden Stratum 20	Shell	6.25	—	4,530 ± 80	4,690 (4,420) 4,180
Beta-185923	3	Midden Stratum 22	Shell	6.8	—	4,980 ± 70	5,270 (4,990) 4,820
SRI AS (Arlington Springs)	1	Soil core surface	Land surface (2008)	0	—	—	—58
2007 AS-568	1	Ab1 horizon	Humic acids	0.36	—	—	4,070 (4,055) 4,040
2007 AS-576	1	Ab2 horizon	Humic acids	207.5	—	—	6,760 (6,740) 6,720
—	4	Living floor midden	Shell	291	—	—	7,190 (7,175) 7,160
—	4	Charcoal	Charcoal	1,249	—	—	11,705 (11,680) 11,655

Note: For study, 1 = This study; 2 = Glassow et al. (2009); 3 = Ballantyne (2006); 4 = J. Johnson, personal communication, 29 May 2009.

<sup>a</sup>Ages of land surfaces and artifacts inferred from historic record and translated into Cal. age BP.

<sup>b</sup>Sedimentation rates calculated from Cal. age BP intercepts of current row and row above in table.

**Table 2.** Soil data from three selected Pozo sites, locations in Figure 2

Depth (cm)	Horizon	Munsell color (dry)	Munsell color (wet)	Texture	Clay (%) <sup>a</sup>	Notes
Pozo 1 midden site						
0–28	Historic sediment	2.5Y6/4	2.5Y5/4	Sil	20	5
28–38	Gravel1	2.5Y5/4	2.5Y3/3	Vgr S	2	
38–45	Gravel2	2.5Y5/4	2.5Y3/3	Xcgr S	1	
45–54	Gravel3	2.5Y4/4	2.5Y3/3	Sl	14	
54–55	Fine buff (Av?)	2.5Y6/4	2.5Y4/4	Sil	20	
55–57	Midden A	2.5Y4/2	2.5Y3/2	Vgr l	16	5
57–85	Ab1	2.5Y4/2	2.5Y3/2	Sicl	30	
85–100	Midden B	2.5Y4/3	2.5Y3/2	Sicl	28	
100–138	Ab2	2.5Y4/3	2.5Y3/3	Sicl	35	
138–149	Midden C	2.5Y4/3	2.5Y3/2	Sicl	30	5
149–175	Ab3	2.5Y4/4	2.5Y3/3	Sicl	30	
175–190	Midden D	2.5Y3/2	10 YR 2/1	Sicl	30	5
190–205	Gravel4	—	—	—	—	
205–220	Dark sands	2.5Y4/3	2.5Y3/2	Sicl	28	
220–245	Light sands	2.5Y4/4	2.5Y4/3	Sl	15	
245–260+	Gravel5	2.5Y5/4	2.5Y4/4	Xgr Sl	12	5
Wetland arroyo wall 1						
0–10	A1	10 YR 5/4	10 YR 3/4	Sl	15	
10–19	A2	10 YR 5/2	10 YR 3/2	Cl	30	
19–108	Btg1	2.5Y7/1	2.5Y5/1	Sic	50	1
108–130	Btg2	2.5Y6/1	2.5Y3/1	Sicl	40	1
130–132	Btg3	2.5Y6/1	2.5Y5/2	Sicl	40	1, 2
132–172	Btg4	2.5Y6/2	2.5Y5/3	Sicl	35	3
172–187+	Btg5	2.5Y6/2	2.5Y4/2	Sic	50	3, 4
Wetland pit 1						
0–5	A1	2.5Y6/3	2.5Y4/3	Cl	30	
5–19	A2	2.5Y5/3	2.5Y3/3	L	20	
19–70	Bt1	2.5Y4/1	2.5Y3/1	Sic	45	1
70–84+	Bt2	2.5Y4/1	2.5Y3/1	Sicl	36	

Note: Cl = clay loam; L = loam; S = sand; Sl = sandy loam; Sic = silty clay; Sicl = silty clay loam; Sil = silty loam; Vgr = very gravelly; Xcgr = extremely gravelly. For notes, 1 = faint redoximorphic features; 2 = white mottling; 3 = redoximorphic features; 4 = below water table; 5 = contains datable marker used in aggradation rate calculations.

<sup>a</sup>Estimated via hand texturing.

initiation of ranching and agricultural activities. To assess the impact and timing of sheep overgrazing with watershed dynamics, we gathered island-wide and pasture-specific sheep population estimates from a variety of sources and converted them to estimates of sheep density per square kilometer. These sources included court records (U.S. District court proceedings), U.S. Coastal Surveys (Alden 1853; Greenwell 1857; W. M. Johnson 1860; Forney 1874–1875), U.S. Bureau of the Census records (1860, 1870), previous studies (Dunkle 1950; Van Vuren 1981; Schuyler 1993), and SCI ranching and hunting records.

We also collected topographic maps and drawings of the Pozo watershed, along with aerial photos dating back to 1929, to provide a time-series of landscape change visualizations. Precipitation records from both SCI (1905–2002) and the city of Santa Barbara

(1867–2007) were also collected and analyzed for unusual patterns during the window of Pozo arroyo initiation. In addition, we scoured nineteenth-century newspaper articles for accounts of SCI news, droughts, and large precipitation events.

### Cosmogenic Radio Nuclide <sup>10</sup>Be Measurements

We collected river-sand samples from four different strata at the Pozo 1 site (the active channel plus three depths exposed in the arroyo wall, at 23 to 38 cm, 38 to 45 cm, and 250 to 265 cm; Figure 5) to determine catchment-mean erosion rates (Granger, Kirchner, and Finkel 1996; von Blanckenburg 2006) using CRN <sup>10</sup>Be inventories. Average basin elevation is 152 m above sea level, and elevation of the Pozo 1 site is 15 m above sea level. The catchment area is 6.47 km<sup>2</sup>. Basin-wide

denudation rates were determined using standard analytical procedures from concentrations of in situ-produced  $^{10}\text{Be}$  in quartz from alluvial sediments (e.g., Kohl and Nishiizumi 1992; von Blanckenburg, Hewawasam, and Kubik 2004; Bookhagen and Strecker 2012). A detailed step-by-step chemical processing manual for in situ CRN can be found at [http://www.geog.ucsb.edu/~bodo/pdf/bookhagen\\_chemSeparation\\_UCSB.pdf](http://www.geog.ucsb.edu/~bodo/pdf/bookhagen_chemSeparation_UCSB.pdf). We used a low-ratio  $^9\text{Be}$  spike ( $^{10}\text{Be}/^9\text{Be}$  ratio of  $\sim 1 \times 10^{-15}$ ). AMS measurements were carried out at Lawrence Livermore National Laboratory. We relied on the original International Chemical and Nuclear Corporation (ICN) standard (Nishiizumi et al. 2007) as reference and used a value of  $5.1 \times 10^{-7} \text{ year}^{-1}$  as decay constant for  $^{10}\text{Be}$ . Production rates were calculated for every 10-m pixel, including variations in altitude, latitude, spallation and muon production, and topographic shielding. Muonogenic production rate calculations were based on formulations and constants described in Granger and Muzikar (2001). We did not find significant differences ( $<5$  percent) compared to the scaling procedure described by Schaller et al. (2001). High-latitude, sea-level (HLSL) spallogenic production rate is  $5.1 \text{ atoms g}^{-1} \text{ year}^{-1}$ . We only included errors associated with AMS errors ( $1\sigma$ ); including errors from production-rate uncertainties would increase errors on average by 15 percent but would not change data interpretation.

### Topographic Measurements

We used airborne and ground-based lidar data from a previous study (Perroy et al. 2010) to derive estimates of volumetric gully erosion in the Pozo watershed and quantify catchment-mean erosion rates in the postarroyo era. We then compared these rates to millennial-timescale catchment-mean erosion rates provided by CRN  $^{10}\text{Be}$  measurements. Airborne lidar data were collected over SCI using the Carnegie Airborne Observatory, an instrument fusing hyperspectral and waveform lidar data with a Global Positioning System–inertial measurement unit (GPS–IMU; Asner et al. 2007; Asner, Hughes, and Vitousek 2008). The instrument was flown at an altitude of 3,000 m above ground level (agl) onboard a Twin Otter aircraft, and the resulting data were processed and precision-corrected to produce a 1.5-m digital elevation model (DEM). This DEM, originally collected for an invasive vegetation species mapping study, was combined with ground-based lidar data collected within the Pozo watershed to obtain

volumetric estimates of soil losses due to historic gully erosion.

## Results

### Field Evidence of the Pozo Pregrazing Environment and Sedimentation Rates

Thick sequences of fluvial sediment, exposed during historic incision of the main channel network, are evident in the arroyo walls of the Pozo watershed (Figure 5). Present down to the channel mouth and progressively thicker and lighter in color in the middle reaches of the floodplain (before thinning out completely upstream), these exposed alluvial sequences generally share the same basic stratigraphy: a series of fine-grained alluvial sediment units that include thick (more than 3 m in places), dark ( $2.5 \text{ Y } 5/2$ , dry), and fine-grained  $A_b$  horizons, occasionally interspersed with intermittent coarser fluvial deposits. Also exposed in the main channel walls are a number of paleochannels filled with coarser fluvial deposits, indicating that the floodplain was occasionally affected by past runoff events that were able to carve out large segments of existing material before back-filling.

Exposed at the top of the arroyo walls, overlying the sedimentary sequence already described, is a buff-colored ( $2.5 \text{ Y } 7/3$ ) silty loam layer, appearing alone or over a series of gravel lenses. This historic sediment layer displays incipient soil development underneath annual grass-dominated vegetation and in places contains buried various ranching artifacts installed after 1853 (Figure 7). As observed in the arroyo walls, this layer generally thickens at tributary junctions and with distance downstream, reaching more than 2 m thick in places. At the tributary junctions, this thickening results from postgrazing historic alluvial fan deposition on the former floodplain surface.

Local sedimentation rates were calculated for the seven different sites on SCI and SRI and are shown in Figure 8. For the three mainstem Pozo arroyo wall sites (Pozo 1, 3, and 7) and the SRI estuary site, there is a sharp increase in sedimentation rates immediately following the introduction of grazing animals in the nineteenth century (black and red arrows). Field evidence of postarroyo aggradation from the Pozo 1 trench shows  $\sim 0.5$  m of aggradation in the main channel since the end of downcutting.

The possibility of intervening scour events between datable markers suggests that calculated sedimentation rates should be considered as minima. In addition, some

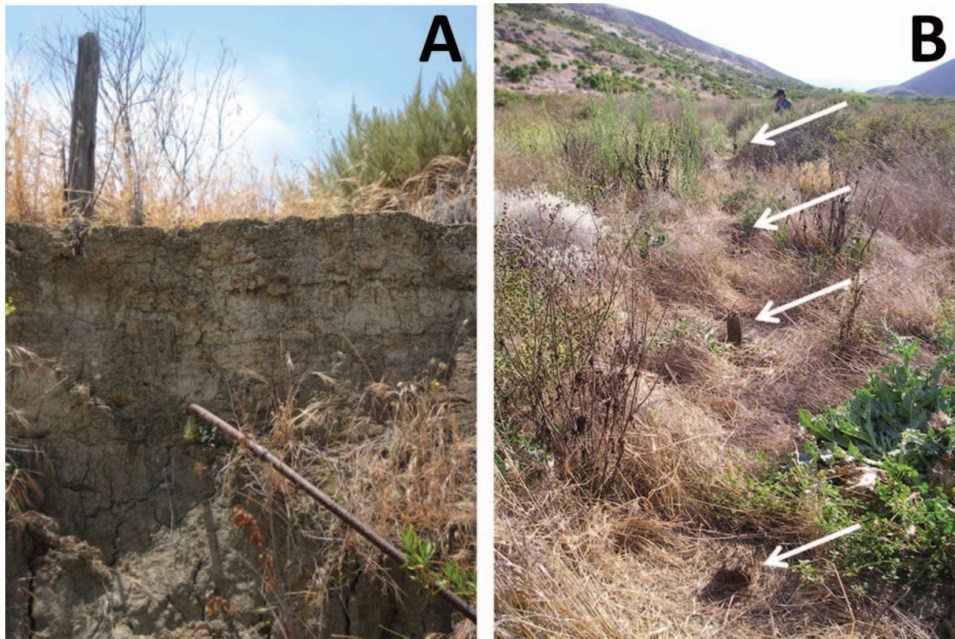


**Figure 7.** (A) Buried water pipe and (B) corral fence posts (tops indicated by white arrows). The water pipe is located at contact between pregrazing surface and overlying postgrazing sediments at arroyo wall near Pozo 3 site. Corral is located nearby on former floodplain surface  $\sim 2$  m above active channel. Fence post woven wire hardware suggests that corral was still in use as late as the 1930s. (Color figure available online.)

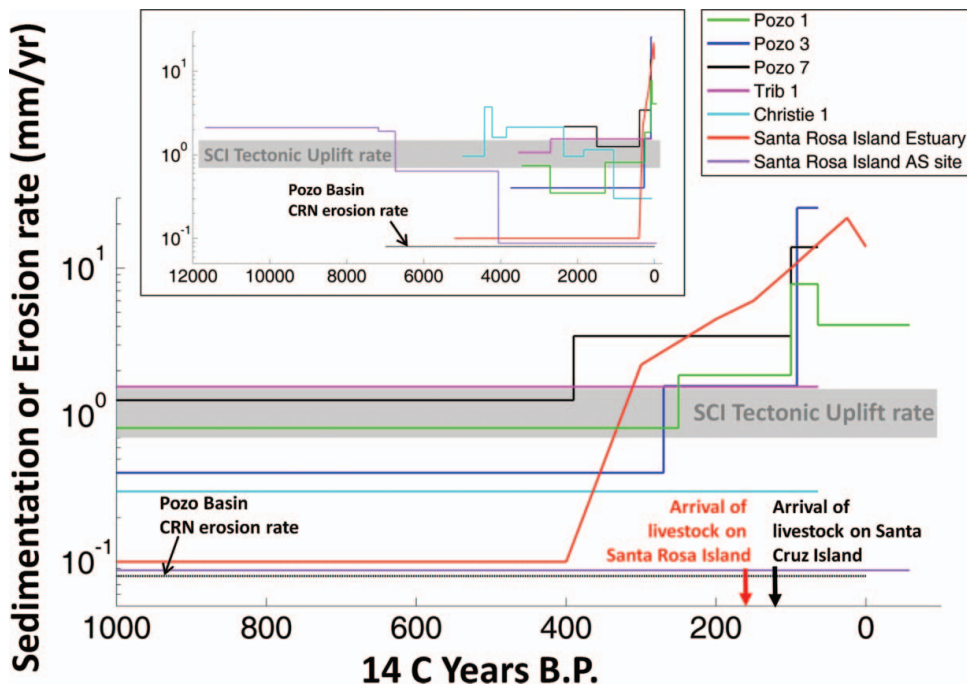


**Figure 8.** Sedimentation rates from seven Channel Island sites, five on southwestern Santa Cruz Island (Pozo 1, Pozo 3, Pozo 7, Trib 1, and Christie 1) and two on Santa Rosa Island: Estuary and Arlington Springs (AS) site. Inset graph is a blow-up of last 1,000 years. Rates calculated from radiocarbon dates of embedded shells, charcoal, and humic acids and historic information for land surfaces and buried artifacts. Long-term Santa Cruz Island tectonic uplift rate taken from Pinter, Sorlien, and Scott (2003) and Chaytor et al. (2008). Santa Rosa Island estuary sedimentation rates from Cole and Liu (1994). CRN = cosmogenic radionuclide. (Color figure available online.)

of the shells were likely transported to their present locations by secondary fluvial processes rather than via primary in situ deposition. If transported, shell ages might not accurately reflect the time of deposition. We acknowledge this possible error source, but the lack of age inversions or shell abrasions or other damage characteristic of transport over long distances suggests that our calculated sedimentation rates are reasonable (see Glassow et al. 2009).

### Data from Historic Documents

We compiled assorted records of the SCI sheep population to plot changes in the density of sheep on the island over time (Figure 3). As the records are estimates of the overall sheep population, derived from the number of sheep collected or shot during round-ups, the data should be interpreted as broadly indicating the number of sheep on the island rather than an accurate count. The late-nineteenth- and early-twentieth-century estimates in particular are suspect and likely low, as there was a large feral population by this period and round-ups were estimated to only capture about 50 percent of the total number of animals (Symmes and Associates 1922). Also shown in Figure 3 are precipitation data (1867–2007) from the city of Santa Barbara, an acceptable longer term proxy as the SCI precipitation record only goes back to 1904 (Brumbaugh 1983).

Following introduction in 1853, the sheep population on SCI rose drastically. By 1875, the sheep density on SCI was nearly seven times the typical mainland stocking rate (Van Vuren 1981; Figure 3). The sharp drop immediately following the 1875 peak comes from a newspaper account as reported by D. L. Johnson (1980), who cited the following from the Santa Barbara Index, March 22, 1877: “twenty-five thousand sheep slaughtered on Santa Cruz Island . . . because of scarcity of food induced by want of rain.”

Two additional stories of interest appeared in the *Santa Barbara Daily Press*, both from 1878 and related to precipitation. The first is a report of an intense SCI rain storm, obtained from the ship *Star of Freedom*.

Terrific rain-storm at Santa Cruz Island, night before last . . . creek became so flooded that it rose ten feet higher than its usual depth. Huge rocks, weighing from two to three tons, were carried into the ocean . . . an old Indian burial ground on the beach, said to be three hundred years old, was completely washed out . . . As the rainfall here (Santa Barbara) was not unusually great, it is probable that Santa Cruz was visited by a friendly waterspout . . .

(“Flood at Santa Cruz Island” 1878, 8)

The second account, also from a newspaper story and dated 30 April 1878, is from a speech to the Santa Barbara Society of Natural History by the French naturalist L. De Cassac. In it, an overview of his geologic research on SCI is presented, along with an explanation that this work was interrupted by “some rare atmospherical circumstances in this climate that had obliged him to modify his itinerary” (“Santa Cruz Island” 1878, 6). This, along with some references made in his notes (Santa Barbara Museum of Natural History), likely refers to the same storm event as reported previously.

From a historic-geomorphic perspective, some of the most valuable documents are a series of maps produced by the U.S. Coast Survey (USCS) in 1860 and 1875 and by the Santa Cruz Island Company (SCIC) in 1886. These maps provide three important snapshots of geomorphic change in Pozo near the beginning of ranching operations (~7,500–15,000 sheep in 1860), at the peak of sheep numbers (~60,000 sheep in 1875), and roughly a decade following this peak. These maps provide several lines of evidence to describe the timing of arroyo incision within Pozo Canyon.

Comparison of the two USCS maps reveals changes in the longitudinal profile of Pozo following sheep introduction. The two maps were georeferenced and the contour lines within the Pozo Canyon floodplain digitized and compared to a total station survey of the Pozo thalweg in 2007 (Figure 9). Differences in contour spacing on USCS maps from 1860 and 1875 indicate that a number of knickpoints had developed on the lower Pozo floodplain by 1875.

The presence or absence of features across the three maps also helps identify the timing of arroyo formation. In neighboring watersheds, both USCS maps clearly show arroyos, yet the channel in Pozo does not appear incised in either map (Figures 9 and 10). In addition, the 1875 map uses a stippled vegetation symbology for some areas along the Pozo channel that can be interpreted as indicating wetter vegetation. This corroborates field observations of relict hydric soil properties (Figure 2, Table 2) and provides additional evidence for a formerly higher water table and the existence of an unincised wetland in this area as late as 1875. In contrast, the 1886 plan for Pozo drawn by the SCIC (Figure 10, upper right) shows several changes to the channel. The pool of standing water near the mouth of the basin shown clearly in 1875 does not appear on the 1886 map. In addition, the number of tributary channels coming into the floodplain just to the east of the corral has increased from two to four. Most important, the 1886 map clearly shows a well-defined boundary along

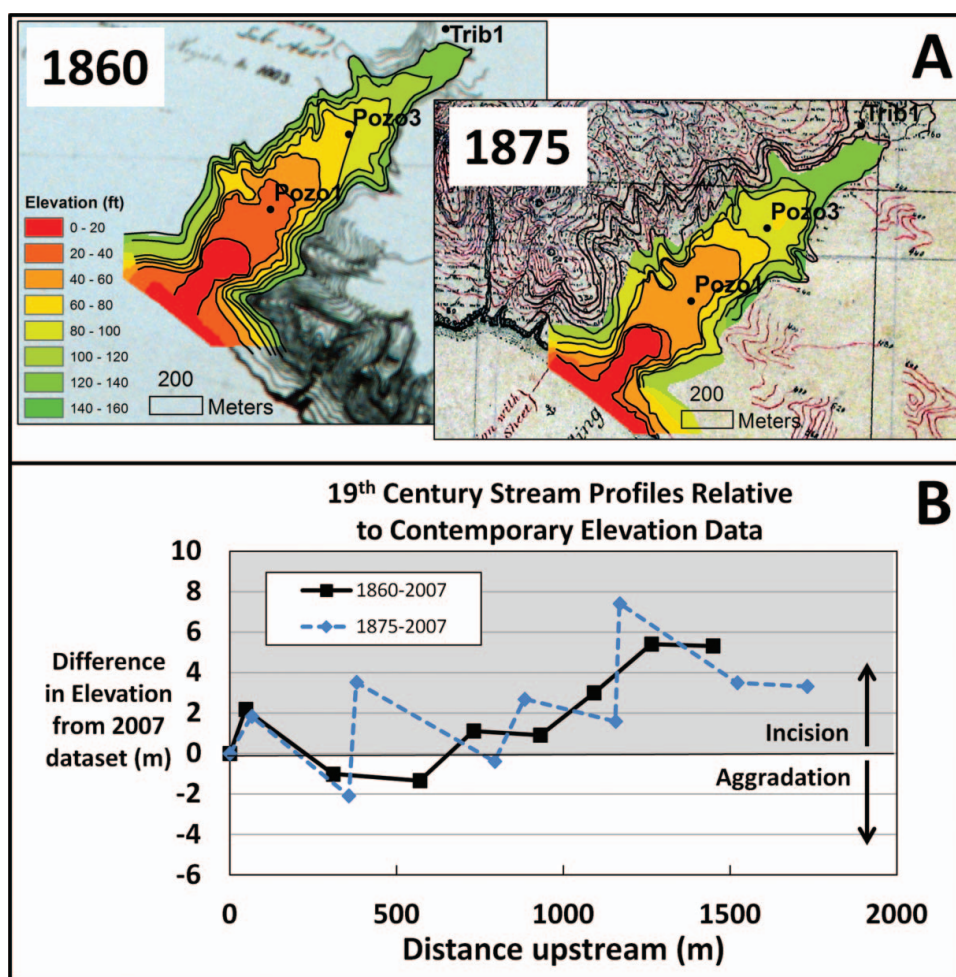


**Figure 9.** (A) 1860 and 1875 U.S. Coast Survey maps with digitized floodplain contours for the lower Pozo watershed. Locations of three sedimentation sites (Pozo 1, Pozo 3, and Trib 1) are also shown. (B) Lower Pozo stream profile plots for 1860 and 1875 maps, relative to 2007 total-station survey data. Relative incision generally increases with distance upstream. (Color figure available online.)

the main channel and some tributaries of the drainage. This channel appears to have swept through the southeastern corner of the agricultural field (indicated by the dashed line).

This cartographic evidence suggests that arroyo formation occurred between 1875 and 1886, which slightly postdates the maximum sheep stocking rate in 1875. Figure 10 (upper left) shows a 2009 aerial image with the present-day lateral extent of the Pozo arroyo as determined from a high-resolution DEM, along with digitized ranching features from the georeferenced 1875 Coastal Survey map (Perroy et al. 2010). The present arroyo cuts through both the historical field and corral (Figure 7), showing that the arroyo continued to impact ranching structures after 1886.

The earliest aerial photo of SCI (1929) shows an extensive and well-established arroyo and gully system

in the Pozo watershed, with gullies occupying virtually every major and minor tributary. In the lower Pozo watershed, over the highly erosive and weakly lithified sedimentary formations, the incised tributary channels are disconnected from the main stem arroyo and terminate on the former floodplain surface. In the middle and upper reaches of the basin, over the more resistant volcanic units, the incised tributaries run directly into the main channel. There is no evidence of significant lateral growth of the system since 1929, although gully deepening and arroyo sidewall collapse are ongoing active processes.

#### CRN $^{10}\text{Be}$ Measurements

Results from the CRN  $^{10}\text{Be}$  measurements, including calculated catchment-mean erosion estimates, are

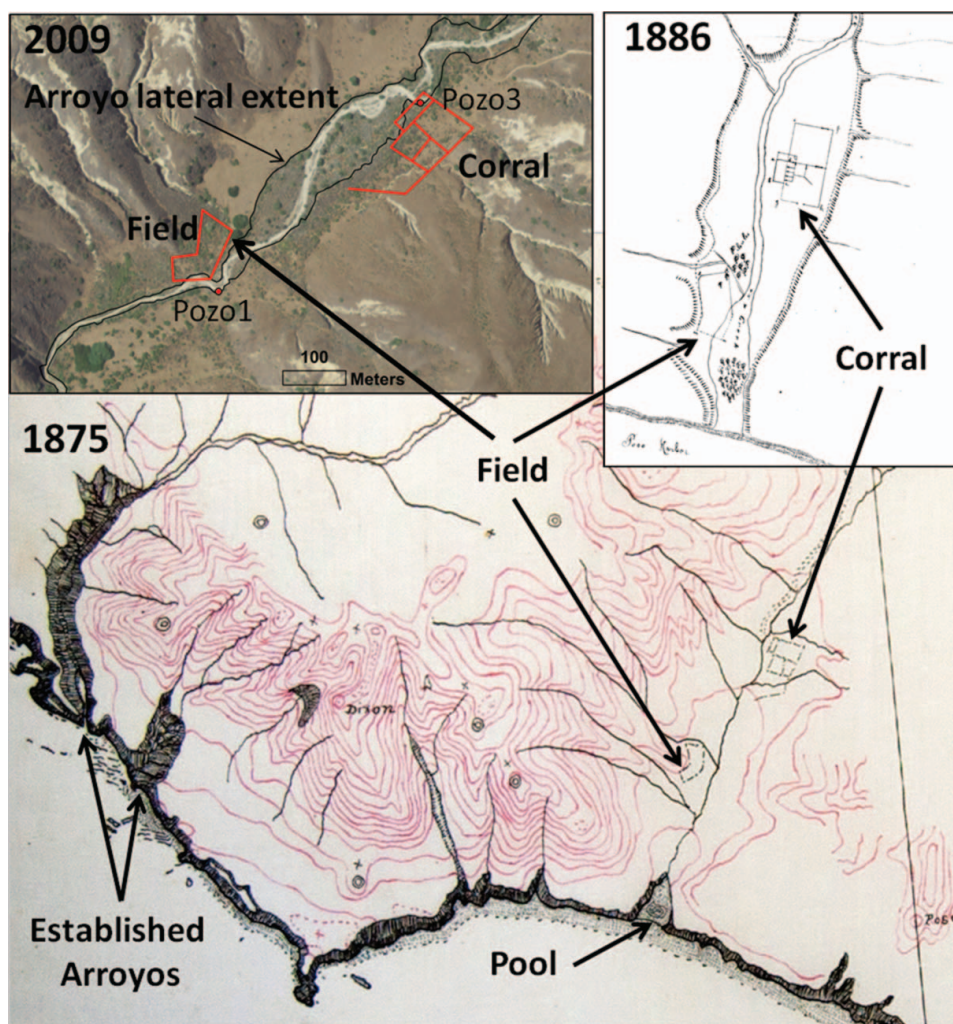


**Figure 10.** 1875 U.S. survey map of lower Pozo floodplain and western coastline (bottom), 1886 sketch of lower Pozo (upper right), and 2009 aerial image (upper left). In the 1875 map, established arroyos are shown in western drainages but absent in Pozo Canyon. In the 1886 sketch, depicted landscape changes include alteration of an agricultural field (by what we interpret as arroyo entrenchment) and an increase in the number of tributaries entering the floodplain east of the corral. In the 2009 image, a digitized outline of arroyo lateral extent from light detection and ranging (lidar) data and cultural features is shown along with Pozo 1 and Pozo 3 (Figure 7) sampling sites. (Color figure available online.)

shown in Table 3. Our catchment-mean erosion rates are generally similar to one another, varying from  $71 \pm 2 \mu\text{m}/\text{year}$  ( $0.07 \text{ mm}/\text{year}$ ; RP401), to  $81 \pm 2 \mu\text{m}/\text{year}$  (RP407), to  $78 \pm 2 \mu\text{m}/\text{year}$  (RP451). The CRN concentrations in river sands give a catchment-mean erosion rate averaging over several millennia. Assuming a landscape in CRN steady state, our erosion rates average over  $\sim 7$  to  $\sim 8.6$  kyr. In other words, this is the time it takes to erode the  $e$ -folding depth of 60 cm ( $160 \text{ g cm}^{-2}/2.65 \text{ g cm}^{-3} \approx 60 \text{ cm}$ ) with the catchment-mean erosion rates. The similarities in the catchment-mean erosion rates throughout the profile from different depths support a CRN steady-

state landscape and a steady erosion rate. The mean erosion rate is  $77 \pm 2 \mu\text{m}/\text{year}$  and averages over the past 7.8 kyr.

### Topographic Measurements

Results from a previous study quantifying gully erosion in a representative Pozo watershed subcatchment produced an erosion factor of  $0.29 \text{ m}^3 \text{ m}^{-2}$  (Perroy et al. 2010). We multiplied this erosion factor by the Pozo watershed area ( $6.46 \times 10^6 \text{ m}^2$ ) to produce a basin-wide estimate of  $1.9 \times 10^6 \text{ m}^3$  of material lost as a result of gully erosion.

**Table 3.** Cosmogenic radionuclide  $^{10}\text{Be}$  accelerator mass spectrometry results and associated parameters

Sample name	Arroyo wall depth (m)	$^{10}\text{Be}/^9\text{Be}$ ratio (corrected for backgrounds)		Sample size (g)	$^{10}\text{Be} \times 10^3$ (atoms per 1 g quartz)	$\pm$	Basin lowering ( $\mu\text{m}/\text{yr}$ )	$\pm$
		Ratio	Error					
RP2-2b	2.5–2.6	No current	No current	87.7	—	—	—	—
RP401	0.1 (active channel)	2.92E-13	7.82E-15	92.9	43.17	1.16	71.3	2
RP407	0.38–0.38	5.27E-13	1.47E-14	139.3	37.88	1.06	81.3	2.3
RP451	0.38–0.45	3.61E-13	1.01E-14	115.1	39.4	1.1	78.2	2.3

## Discussion

For millennia prior to the introduction of grazing animals, the Pozo watershed was relatively stable. Although tectonic uplift raised the basin  $\sim 4$  to 9 m in the 6,000 years following sea-level stabilization, thick sequences of  $A_b$  horizons in the stratigraphic record suggest that this was a period of stability and slow floodplain sedimentation (Zielhofer et al. 2002; Buol et al. 2003; Daniels 2003). Paleoclimatic conditions within the mid- to late-Holocene period (warmer and drier relative to the Pleistocene and early Holocene) were also conducive to sedimentation (Heusser 1978; Cole and Liu 1994; Kirby et al. 2007; Kirby et al. 2010).

In contrast, evidence from the period following the onset of sheep grazing in 1853 provides a record of accelerated geomorphic change. Increases in runoff, hillslope erosion, and floodplain deposition were largely driven by the extensive vegetation denudation and soil disturbance associated with a dramatic and unsustainable rise in the island's sheep population. The effects of these changes were amplified by secular variations in climate, namely, the drought of 1877 (which further suppressed the already degraded vegetation cover) and higher than average rains in 1878 (Figure 3, inset). Newspaper records support these abnormally high precipitation data, including multiple accounts of a large storm in 1878, occurring within the 1875 and 1886 window of arroyo incision suggested by the map record. Although other causes for arroyo initiation (including earthquake activity) cannot be completely ruled out, the power of single storm events to produce dramatic landscape changes has been well documented (Lamb and Fonstad 2010).

### Arroyo Formation in Threshold Landscapes

Landscape response to environmental change is a basic tenet of geomorphology. Thus, a majority of work in

geomorphic evolution has been associated with understanding the effects of external forcings such as climate change, tectonics, and base-level or sea-level changes (which themselves might be interrelated; Bull 1991). Many of the models invoking external explanations for arroyo formation have at their heart the same set of processes (Figure 11A). A decrease in vegetation density, caused by some external forcing mechanism, produces increased overland flow during storm events. This leads to enhanced soil erosion, further reducing the vegetation density and increasing the sediment concentration of the water. In response, the downstream fluvial system adjusts through aggradation and storage of the eroded sediments from the hillslopes. As the reservoir of soil available for erosion is depleted, runoff increases and the sediment concentration of the water decreases, increasing its capacity to do geomorphic work. Eventually the threshold of critical stream power is exceeded and channel degradation or incision begins. Base-level lowering due to climatic changes or tectonic events can produce similar changes.

The predictive power of these external arroyo formation models can be increased if the concept of an internal geomorphic threshold is included (Schumm 1973). This concept is illustrated by Figure 11B, depicting a hypothetical relation between valley-floor gradient and instability through time. As time passes, the valley floor becomes increasingly unstable due to continued sedimentation with sediment material characterized by low cohesion, eventually leading to an oversteepening of the valley floor. Individual storm events might temporarily raise the degree of instability as indicated by the vertical lines. A small storm event could trigger massive changes in one watershed and a 1,000-year flood might do little long-lasting work in another, depending on how far each is from its internal geomorphic threshold. One of the impressive products of this theoretical framework is its ability to explain why neighboring watersheds might respond differently to the same external

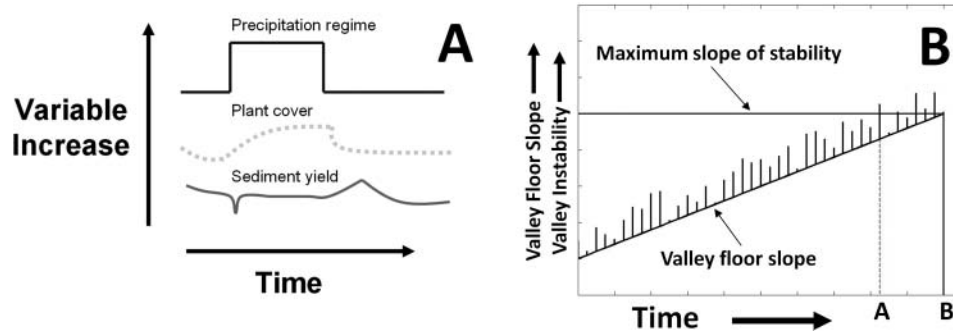


**Figure 11.** (A) Model of biogeomorphic response of plant cover and sediment yield for rocky southwestern U.S. hillslope subsystems to abrupt changes in climate. Modified from Knox (1972) and Bull (1991). (B) Hypothetical relation between valley-floor slope/instability and time. Black vertical lines represent instability created by individual flood events. Where the valley floor slope meets the maximum slope of stability (Time B), valley floor failure or trenching will occur. Failure might also occur earlier due to increased instability from an individual storm event (Time A). Modified from Schumm (1973).

forces, possibly explaining the patchwork of arroyos on southwestern SCI at the onset of grazing (Figure 10). In other words, the system's internal natural variability in vegetation cover, soil depth, volume of sediment stored on the hillslopes, channel length, and channel width result in different triggering thresholds. Ultimately this leads to a landscape with asynchronous arroyo formation despite similar external forcing factors.

### Arroyo Formation in the Pozo Watershed

We argue that the Pozo watershed was approaching its intrinsic geomorphic threshold for arroyo formation prior to the advent of grazing due to millennia of sedimentation in response to mid-Holocene sea-level rise but maintain that the timing of incision was accelerated by the disturbance and vegetation removal caused by sheep overgrazing and ultimately triggered by a drier than average year followed by a large flood event in 1878. These changes correspond to work associating abrupt transitions from multiyear droughts to lengthy periods of above-average precipitation and other climate variations with strong impacts on hillslope erosion and arroyo dynamics in the Colorado Plateau (Hereford 2002; McAuliffe, Scuderi, and McFadden 2006). These changes also reduced forage for grazing and impeded movement between the field and corral, negatively impacting ranching activities. A reconstruction of geomorphic change for the period covered in this study is shown in Figure 12.

Although hillslope disturbance increased very rapidly following the introduction of grazing animals, the Pozo watershed would have eventually aggraded to its point of instability even in their absence. The

introduction of grazers only served to speed up that process. Assuming that the height of the arroyo wall represents the point of instability beyond which arroyo incision was only one large storm event away, it is possible to extrapolate the pregrazing sedimentation rate data to determine when arroyo incision would have occurred in the absence of grazing. This exercise was conducted for the Pozo 1 site, using the average (minimum/maximum) pregrazing sedimentation rates 0.3 (0.9/1.9; mm/year) and the thickness of the sediment above the 1850 pre-postgrazing stratigraphic boundary (280 mm) as the amount of sedimentation necessary to reach potential instability. Based on these rates, arroyo entrenchment would have occurred sometime around the year 2161 (1997/2783) AD. Actual entrenchment, circa 1878, happened 283 years earlier than this calculated average. Even using the minimum rate, entrenchment occurred more than a century earlier than expected due to changing external forcing factors. Although the selection of Pozo 1 as the location for initial valley floor gully incision is arbitrary, it is almost certain that grazing activity sharply accelerated the watershed's geomorphic transition from sedimentation to degradation, potentially by a century or more.

### Comparison of Pre- and Postgrazing Basin-Wide Erosion Estimates

We took advantage of previous work measuring volumetric gully erosion in the Pozo watershed in an attempt to quantify the difference in catchment-mean erosion rates between the pre- and postgrazing eras. That work, based on high-resolution lidar data, provided a basin-wide estimate of  $1.9 \times 10^6 \text{ m}^3$  (or

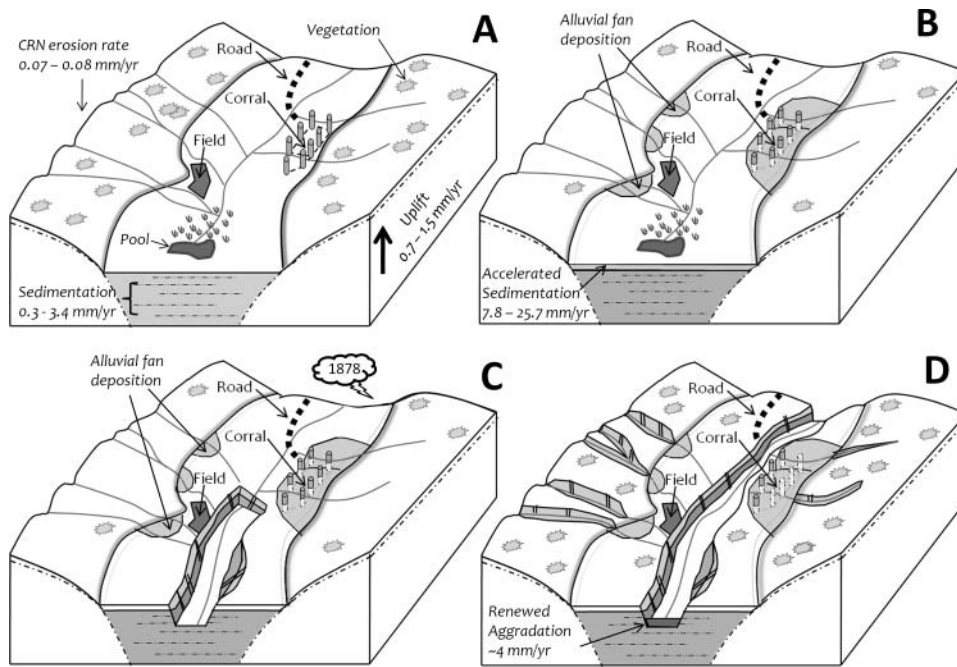


**Figure 12.** Reconstruction of landscape evolution in the Pozo watershed on Santa Cruz Island. (A) Immediately following establishment of ranching activities: Landscape has yet to respond to disturbance and is still slowly aggrading as it had been for the past millennia. (B) Nearly coeval vegetation denudation from overgrazing and alluvial fan formation led to accelerated sedimentation in the valley bottom. (C) Initial arroyo incision, likely triggered by 1878 storm, propagates upstream toward the catchment's headwaters. (D) Fully developed arroyo entrenchment in the main and tributary channels, renewed aggradation in the main channel, and revegetation in the absence of grazing pressure. CRN = cosmogenic radionuclide.

$0.29 \text{ m}^3 \text{ m}^{-2}$ ) of material lost as a result of gully erosion since the mid-nineteenth century (Perroy et al. 2010). These values are similar to the results of other recent work estimating gully erosion volumes from active gullies (Wu et al. 2008; Marzloff and Poesen 2009). Using the estimate for the  $6.47 \text{ km}^2$  Pozo watershed, and the amount of time elapsed between lidar data collection and the likely date of arroyo incision in 1878 (132 years), we calculated a postgrazing catchment-mean erosion rate of  $2.2 \text{ mm/year}$ . This is roughly thirty times greater than our averaged pregrazing CRN catchment-mean erosion rate of  $0.076 \pm 2 \text{ mm/year}$  with a characteristic timescale of 7.6 kyr. This estimate is likely low, as the aerial photo record for SCI shows essentially no lateral extension of the gully network following 1929. Using a shorter incision interval of 1878 to 1929 (fifty-one years), the erosion rate in the basin increases to  $5.7 \text{ mm/year}$ . If a similar amount of gully erosion occurred over 1,000 years, rather than over the shorter time frames suggested here, the erosion rate would still be  $0.3 \text{ mm/year}$ . Following disturbance, sediment yields in perturbed drainage basins in the American Southwest have been shown to behave in a predictable manner, initially spiking before achieving

a new condition of relative stability within about 100 years (Schumm, Harvey, and Watson 1984).

## Conclusions

Arroyo formation is an abrupt and highly destructive process with major geomorphic, hydrologic, infrastructural, and agricultural consequences. As such, arroyo cutting has often been framed in the past as a sudden and direct response to an external change, either climate or human induced. With new data sets and advances in measuring environmental change over long timescales, we can now view arroyos as part of a larger and more complex geomorphic process of equilibrium adjustment, incorporating interactions and feedbacks between virtually all aspects of physical geography. Appreciation of this complexity calls for reevaluation of our understanding of the widespread arroyo cutting that occurred around the world in the nineteenth century, including the need for more complete, detailed data sets to explain the responses of individual watersheds.

Pozo Canyon on southwestern SCI is a unique case. The timing and main drivers of arroyo incision

(vegetation removal due to severe sheep overgrazing in combination with short-term climate fluctuations) are well constrained, and we can quantify geomorphic changes in the watershed through a rich datable stratigraphic record and CRN- and lidar-derived estimates of pre- and postgrazing catchment-mean erosion rates. These data can also provide a vision of what the canyon would have looked like in the absence of grazing and what it will become in the near future. Had grazing animals never been introduced to the Pozo watershed, it would likely have remained a nonincised valley with an extensive lower wetland experiencing continued slow sedimentation for another century or more before inevitable arroyo incision. Had there been no large storm or other event around 1878, the valley might have held on for an indeterminate length of time under overgrazing pressure. The signs of imbalance were already evident on historic maps, however—and written in the stories of other hillsides, grazed and ungrazed, across SCI and the Southwestern United States. Under the current conditions it is likely that complex stream response adjustments will persist, continued revegetation will decrease hillslope sediment yields and slow overall sedimentation rates, and the lower wetland will eventually reestablish. We argue that this catchment, with its multiple lines of geomorphic evidence dating back to the mid-Holocene, represents a valuable contribution to arroyo formation studies.

## Acknowledgments

We would like to thank Sharon Dansereau and three anonymous reviewers for their insightful comments and valuable suggestions; The Nature Conservancy and the University of California Natural Reserve System for access to southwestern Santa Cruz Island; Mike Glasgow, Dan Muhs, Lyndal Laughrin, and John Johnson for their expertise and time; Greg Asner and the Carnegie Airborne Observatory team for use of their lidar data; and the many people who contributed out in the field. The research described in this article has been funded in part by the W. M. Keck Foundation, Gordon and Betty Moore Foundation, Carnegie Institution, William Hearst III, and the U.S. Environmental Protection Agency (EPA) under the Science to Achieve Results (STAR) Graduate Fellowship Program. The EPA has not officially endorsed this publication and the views expressed herein might not reflect the views of the EPA.

## References

- Alden, J. 1853. Report of Lieut. Comg. James Alden, U.S. Navy, assistant in the Coast Survey, to the Superintendent, on the reconnaissance of the Western coast from San Francisco, south, to San Diego, including the Santa Barbara islands and channel. In *Report of the Superintendent of the Coast Survey showing the progress of the survey during the year 1852*, ed. A. D. Bache, 104–07. Washington, DC: Robert Armstrong.
- Allen, C. D., and D. D. Breshears. 1998. Drought-induced shift of a forest–woodland ecotone: Rapid landscape response to climate variation. *Proceedings of the National Academy of Science (USA)* 95:14839–42.
- Antevy, E. 1952. Arroyo-cutting and filling. *Journal of Geology* 60:375–85.
- Asner, G. P., R. F. Hughes, and P. M. Vitousek. 2008. Invasive plants transform the three dimensional structure of rain forests. *Proceedings of the National Academy of Science* 105:4519–23.
- Asner, G. P., D. E. Knapp, M. O. Jones, T. Kennedy-Bowdoin, R. E. Martin, J. Boardman, and C. B. Field. 2007. Carnegie Airborne Observatory: In-flight fusion of hyperspectral imaging and waveform light detection and ranging (wLiDAR) for three-dimensional studies of ecosystems. *Journal of Applied Remote Sensing* 1: 1–21.
- Bai, Z. G., D. L. Dent, L. Olsson, and M. E. Schaepman. 2008. Global assessment of land degradation and improvement identification by remote sensing. Report 2008/FAO/ISRIC, UN Food and Agriculture Organization, Rome, Italy.
- Ballantyne, K. E. 2006. An analysis of buried archaeological sites on western Santa Cruz Island, California. Unpublished thesis, University of California, Santa Barbara.
- Bancroft, H. H. 1886. *History of California*. San Francisco: The History Company.
- Bard, E., B. Hamelin, R. G. Fairbanks, and A. Zindler. 1990. Calibration of the 14-C timescale over the past 30,000 years using mass spectrometric U-Th ages from Barbados corals. *Nature* 345:405–09.
- Bayon, B., B. Dennielou, J. Etoubleau, E. Ponzevera, S. Toucanne, and S. Bermell. 2012. Intensifying weathering and land use in iron age central Africa. *Science* 335:1219–22.
- Bickel, P. M. 1978. Changing sea levels along the California coast: Anthropological implications. *The Journal of California Anthropology* 5:6–20.
- Bookhagen, B., H. P. Echter, D. Melnick, M. R., Strecker, and J. Q. G. Spencer. 2006. Using uplifted Holocene beach berms for paleoseismic analysis on the Santa Maria Island, south-central Chile. *Geophysical Research Letters* 33:L15302.
- Bookhagen, B., and M. R. Strecker. 2012. Spatiotemporal trends in erosion rates across a pronounced rainfall gradient: Examples from the southern Central Andes. *Earth and Planetary Science Letters* 327–328:97–110.
- Brumbaugh, R. W. 1980. Recent geomorphic and vegetal dynamics on Santa Cruz Island, California. In *The California islands: Proceedings of a multidisciplinary symposium*, ed. D. M. Power, 139–58. Santa Barbara, CA: Santa Barbara Museum of Natural History.

- . 1983. Hillslope gullying and related changes: Santa Cruz Island, California. Unpublished PhD dissertation, University of Southern California at Los Angeles.
- Bryan, K. 1925. Date of channel trenching (arroyo cutting) in the arid Southwest. *Science* 62:338–44.
- Bull, W. B. 1991. *Geomorphic responses to climatic change*. New York: Oxford University Press.
- . 1997. Discontinuous ephemeral streams. *Geomorphology* 19:227–76.
- Buol, S. A., R. J. Southard, R. C. Graham, and P. A. McDaniel. 2003. *Soil genesis and classification*. Ames: Iowa State University Press.
- Chaytor, J. D., C. Goldfinger, M. A. Meiner, G. J. Huftile, C. G. Rosmos, and M. R. Legg. 2008. Measuring vertical tectonic motion at the intersection of the Santa Cruz–Catalina Ridge and Northern Channel Islands platform, California Continental Borderland, using submerged paleoshorelines. *Geological Society of America Bulletin* 120 (7–8): 1053–71.
- Cole, K. L., and G. W. Liu. 1994. Holocene paleoecology of an estuary on Santa Rosa Island, California. *Quaternary Research* 41:326–35.
- Colvin, W., and S. Gliessman. 2000. Fennel (*Foeniculum vulgare*) management and native species enhancement on Santa Cruz Island, CA. In *The Fifth California Islands Symposium*, ed. D. R. Browne, K. L. Mitchell, and H. W. Chaney, 184–89. Washington, DC: Minerals Management Service, U.S. Department of the Interior.
- Cooke, R. U., and R. W. Reeves. 1976. *Arroyos and environmental change*. Oxford, UK: Oxford University Press.
- Dadson, S. J., N. Hovius, H. Chen, B. Dade, M. L. Hsieh, S. D. Willett, and J. C. Hu, et al. 2003. Links between erosion, runoff variability and seismicity in the Taiwan orogen. *Nature* 426:648–51.
- Daniels, M. 2003. Floodplain aggradation and pedogenesis in a semiarid environment. *Geomorphology* 56:225–42.
- Dibblee, T. W. 2001. Geologic map of western Santa Cruz Island, Santa Barbara, California. Dibblee Geological Foundation Map #DF-77. Santa Barbara, CA: Dibblee Geological Foundation.
- Dodge, R. E. 1902. Arroyo formation. *Science* 15:746.
- Dunkle, M. B. 1950. *Plant ecology of the Channel Islands of California*. Allan Hancock Pacific Expeditions 13(3). Los Angeles: University of Southern California Press.
- Elliott, J. G. 1979. Evolution of large arroyos, the Rio Puerco of New Mexico. Unpublished master's thesis, Colorado State University, Fort Collins, CO.
- Elliott, J. G., A. C. Gellis, and S. B. Aby. 1999. Evolution of arroyos: Incised channels of the southwestern United States. In *Incised river channels: Processes, forms, engineering and management*, ed. S. E. Darby, and A. Simon. New York: Wiley.
- Erlandson, J. M., T. C. Rick, and R. Vellanoweth. 2004. Human impacts on ancient environments: A case study from California's Northern Channel Islands. In *Voyages of discovery: The archaeology of islands*, ed. S. M. Fitzpatrick, 51–85. Westport, CT: Greenwood.
- Fairbanks, R. G. 1989. A 17,000 year glacio-eustatic sea level record: Influence of glacial melting rates on the Younger Dryas event and deep ocean circulation. *Nature* 342:637–42.
- Fanning, P. C. 1999. Recent landscape history in arid western NSW, Australia: A model for regional change. *Geomorphology* 29:191–209.
- Faulkner, K. R., and C. C. Kessler. 2011. Live capture and removal of feral sheep from eastern Santa Cruz Island, California. In *Island invasives: Eradication and management*, ed. C. R. Veitch, M. N. Clout, and D. R. Towns, 131–34. Gland, Switzerland: IUCN.
- Flood at Santa Cruz Island. 1878. *Santa Barbara Daily Press* 16 February:8.
- Forney, S. 1874–1875. Topographic map of Santa Cruz Island. *US Coast Survey Records*, National Archives, College Park, MD.
- Fox, R. 2000. Agriculture and rural development. In *The geography of South Africa in a changing world*, ed. R. Fox and K. Rowntree, 211–32. Cape Town, South Africa: Oxford University Press.
- Gabet, E. J., and T. Dunne. 2002. Landslides on coastal sage scrub and grassland hillslopes in a severe El Niño winter: The effects of vegetation conversion on sediment delivery. *Geological Society of America Bulletin* 114 (8): 983–90.
- Glassow, M. A. 2002. Prehistoric chronology and environmental change at the Punta Arena site, Santa Cruz Island, California. In *Proceedings of the Fifth California Islands Symposium*, ed. D. R. Browne, K. L. Mitchell, and H. W. Chaney, 555–62. Santa Barbara, CA: Santa Barbara Museum of Natural History.
- Glassow, M. A., O. A. Chadwick, R. L. Perroy, and J. T. Howarth. 2009. Alluvial history and human prehistory in Pozo Canyon, Santa Cruz Island, California. In *Proceedings of the Seventh California Islands Symposium*, ed. C. C. Damiani and D. K. Garcelon, 53–65. Arcata, CA: Institute for Wildlife Studies.
- Goudie, A. S. 2006. Global warming and fluvial geomorphology. *Geomorphology* 79:384–94.
- Graham, M. H., P. K. Dayton, and J. M. Erlandson. 2003. Ice ages and ecological transitions on temperate coasts. *Trends in Ecology and Evolution* 18:33–40.
- Granger, D. E., J. W. Kirchner, and R. Finkel. 1996. Spatially averaged long-term erosion rates measured from in-situ produced cosmogenic nuclides in alluvial sediment. *Journal of Geology* 104:249–57.
- Granger, D. E., and P. Muzikar. 2001. Dating sediment burial with cosmogenic nuclides: Theory, techniques, and limitations. *Earth and Planetary Science Letters* 188 (1–2): 269–81.
- Greenwell, W. E. 1857. *Report of the Superintendent of the U.S. Coast Survey, showing the progress of the survey during the year 1857*. Appendix No. 44: 392–94. <http://docs.lib.noaa.gov/rescue/cgs/001.pdf/CSC-0006.pdf> (last accessed 20 August 2012).
- Hereford, R. 2002. Valley-fill alluviation during the Little Ice Age (ca. A.D. 1400–1880), Paria River basin and southern Colorado Plateau, United States. *GSA Bulletin* 114:1550–63.
- Heusser, L. 1978. Pollen in the Santa Barbara Basin, California: A 12,000-yr record. *Geological Society of America Bulletin* 89:673–78.
- Hochberg, M. C., S. A. Junak, and R. N. Philbrick. 1980. Botanical study of Santa Cruz Island for the Nature Conservancy. Unpublished report. Santa Barbara Botanic Garden, Santa Barbara, CA.

- Howarth, J. T., and L. L. Laughrin. 2009. Many small becoming many large: Understanding changes in cultural landscapes. In *Proceedings of the Seventh California Islands Symposium*, ed. C. C. Damiani and D. K. Garcelon, 89–98. Arcata, CA: Institute for Wildlife Studies.
- Inman, D. L. 1983. Application of coastal dynamics to the reconstruction of palaeocoastlines in the vicinity of La Jolla. In *Quaternary coastlines and marine archaeology*, ed. P. M. Masters and N. C. Fleming, 1–49. New York: Academic.
- Johnson, D. L. 1980. Episodic vegetation stripping, soil erosion, and landscape modification in prehistoric and recent historic time, San Miguel Island, California. In *The California islands: Proceedings of a multidisciplinary symposium*, ed. D. M. Power, 103–21. Santa Barbara, CA: Santa Barbara Museum of Natural History.
- . 1983. The California continental borderland: Landbridges, watergaps and biotic dispersals. In *Quaternary coastlines and marine archaeology: Towards the prehistory of land bridges and continental shelves*, ed. P. M. Masters and N. C. Fleming, 481–527. New York: Academic.
- Johnson, W. M. 1860. Topographic map of Santa Cruz Island, T-1003. U.S. Coast Survey Records, NOAA's Historic Coast & Geodetic Survey (C&GS) Collection, National Archives, Records of the Coast and Geodetic Survey, College Park, MD.
- Junak, S., T. Ayers, R. Scott, D. Wilken, and D. Young. 1995. *A flora of Santa Cruz Island*. Santa Barbara, CA: Santa Barbara Botanic Garden.
- Kennett, D. J. 2005. *The island Chumash: Behavioral ecology of a maritime society*. Berkeley: University of California Press.
- Kirby, M. E., S. P. Lund, M. A. Anderson, and B. W. Bird. 2007. Insolation forcing of Holocene climate change in Southern California: A sediment study from Lake Elsinore. *Journal of Paleolimnology* 38:395–417.
- Kirby, M. E., S. P. Lund, W. P. Patterson, M. A. Anderson, B. W. Bird, L. Ivanovici, P. Monarrez, and S. Nielsen. 2010. A Holocene record of Pacific Decadal Oscillation (PDO)-related hydrologic variability in Southern California (Lake Elsinore, CA). *Journal of Paleolimnology* 44:819–39.
- Knox, J. C. 1972. Valley alluviation in southwestern Wisconsin. *Annals of the Association of American Geographers* 62:401–10.
- . 1977. Human impacts on Wisconsin stream channels. *Annals of the Association of American Geographers* 67:323–42.
- . 1987. Historical valley floor sedimentation in the upper Mississippi Valley. *Annals of the Association of American Geographers* 77:224–44.
- . 2006. Floodplain sedimentation in the Upper Mississippi Valley: Natural versus human accelerated. *Geomorphology* 79:286–310.
- Kohl, C. P., and K. Nishiizumi. 1992. Chemical isolation of quartz for measurement of in situ-produced cosmogenic nuclides. *Geochimica et Cosmochimica Acta* 56:3583–87.
- Lal, R. 2003. Soil erosion and the global carbon budget. *Environment International* 29:437–50.
- Lamb, M. P., and M. A. Fonstad. 2010. Rapid formation of a modern bedrock canyon by a single flood event. *Nature Geoscience* 3:477–81.
- Leopold, L. B., and J. P. Miller. 1956. Ephemeral streams, hydraulic factors and their relation to the drainage net. USGS Professional Paper 282-A. <http://pubs.er.usgs.gov/publication/pp282A> (last accessed 20 August 2012).
- Marston, R. A. 2010. Geomorphology and vegetation on hillslopes: Interactions, dependencies, and feedback loops. *Geomorphology* 116 (3-4): 206–17.
- Marzoff, I., and J. Poesen. 2009. The potential of 3D gully monitoring with GIS using high resolution aerial photography and a digital photogrammetry system. *Geomorphology* 111:48–60.
- McAuliffe, J. R., L. A. Scuderi, and L. D. McFadden. 2006. Tree-ring record of hillslope erosion and valley floor dynamics: Landscape responses to climate variation during the last 400 yr in the Colorado Plateau, northeastern Arizona. *Global and Planetary Change* 50 (3-4): 184–201.
- Meyer, D. F. 1986. Arroyo development, bedload transport, and channel pattern: Experimental and field studies. Unpublished PhD dissertation, Colorado State University, Fort Collins, CO.
- Montgomery, D. R. 2007. *Dirt: The erosion of civilization*. Berkeley: University of California Press.
- Nardin, T. R., R. H. Osborn, D. J. Bottjer, and R. C. J. Scheidemann. 1981. Holocene sea-level curves for Santa Monica shelf, California continental borderland. *Science* 213:331–33.
- Nishiizumi, K., M. Imamura, M. W. Caffee, J. R. Southon, R. C. Finkel, and J. McAninch. 2007. Absolute calibration of <sup>10</sup>Be AMS standards. *Nuclear Instruments and Methods in Physics Research Section B: Beam Interactions with Materials and Atoms* 258 (2): 403–13.
- Orr, P. C. 1962. The Arlington spring site, Santa Rosa Island, California. *American Antiquity* 27 (3): 417–19.
- Patton, P. C., and P. J. Boison. 1986. Processes and rates of formation of Holocene alluvial terraces in Harris Wash, Escalante River basin, south-central Utah. *Geological Society of America Bulletin* 97:369–78.
- Patton, P. C., and S. A. Schumm. 1981. Ephemeral stream processes: Implications for studies of Quaternary valley fills. *Quaternary Research* 15:24–43.
- Perroy, R. L., B. Bookhagen, G. P. Anser, and O. A. Chadwick. 2010. Comparison of gully erosion estimates using airborne and ground-based LiDAR on Santa Cruz Island, California. *Geomorphology* 118:288–300.
- Pinter, N., C. C. Sorlien, and A. T. Scott. 2003. Fault-related fold growth and isostatic subsidence, California Channel Islands. *American Journal of Science* 303:300–18.
- Pinter, N., and W. D. Vestal. 2005. El Niño-driven landsliding and post-grazing recovery, Santa Cruz Island, California. *Journal of Geophysical Research* 110:F2.
- Porcasi, P., J. F. Porcasi, and C. O'Neill. 1999. Early Holocene coastlines of the California Bight: The Channel Islands as first visited by humans. *Pacific Coast Archaeological Society Quarterly* 35:1–24.
- Prosser, I. P., I. D. Rutherford, J. M., Olley, W. J. Young, P. J. Wallbrink, and C. J. Moran. 2001. Large-scale patterns of erosion and sediment transport in river networks, with examples from Australia. *Marine and Freshwater Research* 52:81–99.
- Ramsey, D. S. L., J. Parkes, and S. A. Morrison. 2009. Quantifying eradication success: The removal of feral pigs from Santa Cruz Island, California. *Conservation Biology* 23 (2): 449–59.

- Roemer, G. W., C. J. Donlan, and F. Courchamp. 2002. Golden eagles, feral pigs, and insular carnivores: How exotic species turn native predators into prey. *Proceedings of the National Academy of Sciences of the United States of America* 99:791–96.
- Santa Cruz Island: Researches of a French savant in the island—Lecture of Mons. L. De Cessac, yesterday, before the Santa Barbara Society of Natural History. 1878. *Santa Barbara Daily Press* 30 April:6.
- Schaller, M., F. von Blanckenburg, N. Hovius, and P. W. Kubik. 2001. Large-scale erosion rates from in situ-produced cosmogenic nuclides in European river sediments. *Earth and Planetary Science Letters* 188:441–58.
- Schumm, S. A. 1973. Geomorphic thresholds and the complex response of drainage systems. In *Fluvial geomorphology*, ed. M. Morisawa, 299–310. Binghamton: State University of New York.
- Schumm, S. A., and R. F. Hadley. 1957. Arroyos and the semi-arid cycle of erosion. *American Journal of Science* 255:161–74.
- Schumm, S. A., M. D. Harvey, and C. C. Watson. 1984. *Incised channels: Initiation, evolution, dynamics, and control*. Littleton, CO: Water Research Publications.
- Schumm, S. A., and R. S. Parker. 1973. Implications of complex response of drainage systems for Quaternary alluvial stratigraphy. *Nature* 243:99–100.
- Schuyler, P. 1993. Control of feral sheep (*Ovis aries*) on Santa Cruz Island, California. In *Third California Islands Symposium—Recent advances in research on the California islands*, ed. F. G. Hochberg, 443–52. Santa Barbara, CA: Santa Barbara Museum of Natural History.
- Spaulding, E. S. 1964. *A brief story of Santa Barbara*. Santa Barbara, CA: Santa Barbara Historical Society.
- Stuiver, M., and H. A. Polach. 1977. Discussion: Reporting <sup>14</sup>C data. *Radiocarbon* 19:355–63.
- Symmes and Associates. 1922. *Report on Santa Cruz Island, Santa Barbara County, California*. San Francisco: Symmes and Associates.
- Timbrook, J. 1993. Island Chumash ethnobotany. In *Archaeology on the northern Channel Islands of California, studies of subsistence, economics, and social organization*, ed. M. A. Glassow, 47–62. Salinas, CA: Coyote Press.
- Timbrook, J., J. R. Johnson, and D. D. Earle. 1982. Vegetation burning by the Chumash. *Journal of California and Great Basin Anthropology* 4:163–86.
- U.S. Bureau of the Census. 1860. *Census of Agriculture, 8th Census of the U.S.* Washington, DC: U. S. Bureau of the Census.
- . 1870. *9th Census of the U.S., v.2: Schedule of agricultural recapitulation, Santa Barbara County* (microfilm). Sacramento: California State Library.
- U.S. Department of Agriculture, National Resources Conservation Service. 2007. *Soil survey of Channel Islands National Park, California*. [http://soils.usda.gov/survey/printed\\_surveys/](http://soils.usda.gov/survey/printed_surveys/) (last accessed 18 April 2007).
- U.S. District Court (San Francisco). 1857. Transcripts of the proceedings, case no.176. Petition of Andres Castillero for the island of Santa Cruz, No. 340SD.
- Van Vuren, D. 1981. *The feral sheep of Santa Cruz Island: Status, impacts and management recommendations*. Santa Barbara, CA: The Nature Conservancy.
- Van Vuren, D., and B. E. Coblenz. 1987. Some ecological effects of feral sheep on Santa Cruz Island, California, USA. *Biological Conservation* 41:253–68.
- von Blanckenburg, F. 2006. The control mechanisms of erosion and weathering at basin scale from cosmogenic nuclides in river sediment. *Earth and Planetary Science Letters* 242:224–39.
- von Blanckenburg, F., T. Hewawasam, and P. Kubik. 2004. Cosmogenic nuclide evidence for low weathering and denudation in the wet, tropical highlands of Sri Lanka. *Journal of Geophysical Research* 109:F03008.
- Waters, M. R., and C. V. Haynes. 2001. Late Quaternary arroyo formation and climate change in the American Southwest. *Geology* 29:399–402.
- Weaver, D. W., and B. Nolf. 1969. Geology of Santa Cruz Island. In *Geology of the Northern Channel Islands: American Association of Petroleum Geologists and Society of Economic Paleontologists and Mineralogists Pacific Section*, ed. D. W. Weaver, D. P. Doerner, and B. Nolf. Special publication, 1:24,000 Scale Map.
- Wu, Y., Y. Zheng, Y. Zhang, B. Liu, H. Cheng, and Y. Wang. 2008. Development of gullies and sediment production in the black soil region of northeastern China. *Geomorphology* 101:683–91.
- Zhang, P., P. Molnar, and W. R. Downs. 2001. Increased sedimentation rates and grain sizes 2–4 Myr ago due to the influence of climate change on erosion rates. *Nature* 410:891–987.
- Zielhofer, C., D. Faust, F. Diaz del Olmo, and R. Baena Escudero. 2002. Sedimentation and soil formation phases in the Ghardimaou Basin (northern Tunisia) during the Holocene. *Quaternary International* 93–94:109–25.

Correspondence: Department of Geography and Earth Science, University of Wisconsin—La Crosse, 1725 State Street, La Crosse, WI 54601, e-mail: rperroy@uwlax.edu (Perroy); Department of Geography, 1832 Ellison Hall, UC Santa Barbara, Santa Barbara, CA 93106-4060, e-mail: bodo@eri.ucsb.edu (Bookhagen); e-mail: oac@geog.ucsb.edu (Chadwick); Department of Geography, Middlebury College, McCardell Bicentennial Hall 329, Middlebury, VT 05753, e-mail: jhowarth@middlebury.edu (Howarth).